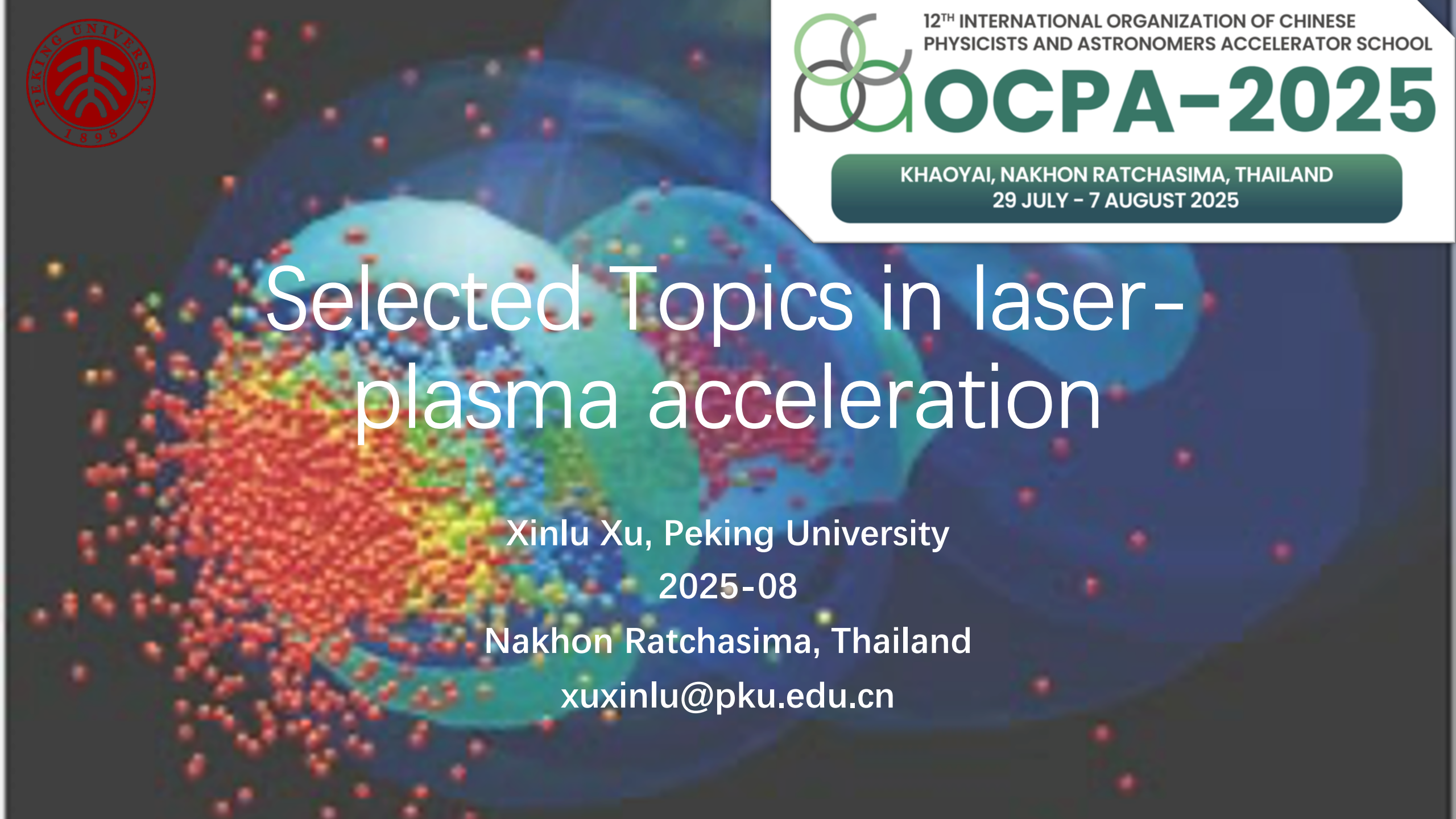

12TH INTERNATIONAL ORGANIZATION OF CHINESE PHYSICISTS AND ASTRONOMERS ACCELERATOR SCHOOL

OCPA-2025

KHAOYAI, NAKHON RATCHASIMA, THAILAND
29 JULY - 7 AUGUST 2025

Selected Topics in laser-plasma acceleration

Xinlu Xu, Peking University

2025-08

Nakhon Ratchasima, Thailand

xuxinlu@pku.edu.cn

Outline

- **Basics of Plasma-based acceleration**
- Injection: high-quality e^- beams
- Applications of plasma-based acceleration

Why using plasma as an acceleration medium?

- The limit of RF technology: **10 ~100 MV/m** because of "breakdown"

  Electrons are "free" in metals.

➢Option 1: material with less free electrons – dielectric: **> GV/m**

➢Option 2: materials with totally free electrons – plasma: no classical breakdown limit, **~ 100 GV/m**

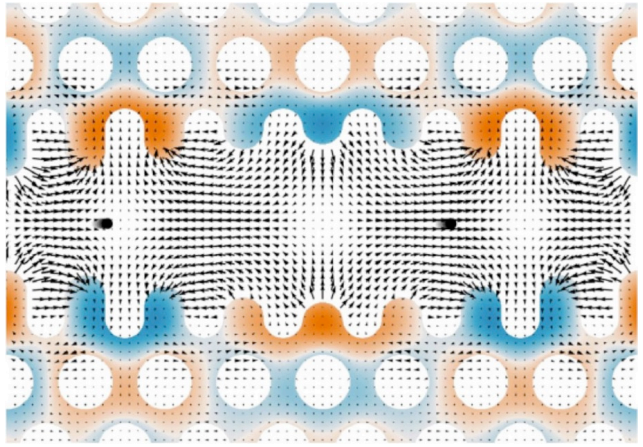

ACHIP – "Accelerator on a Chip"

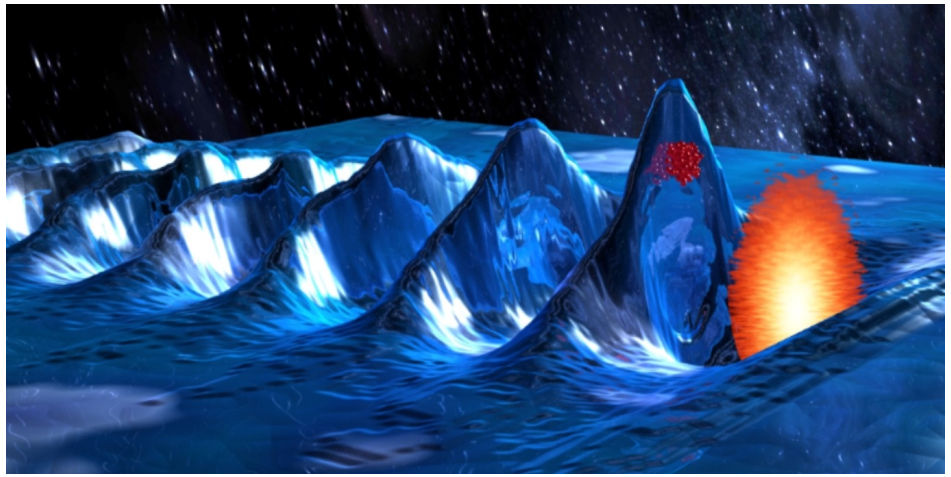

Laser wakefield accelerator (LWFA)

Why using plasma as an acceleration medium?

- Plasma: positive ions and negative electrons, they have equal distribution at equilibrium.
- Plasma oscillation (Langmuir oscillation): collective motion of charged particles.

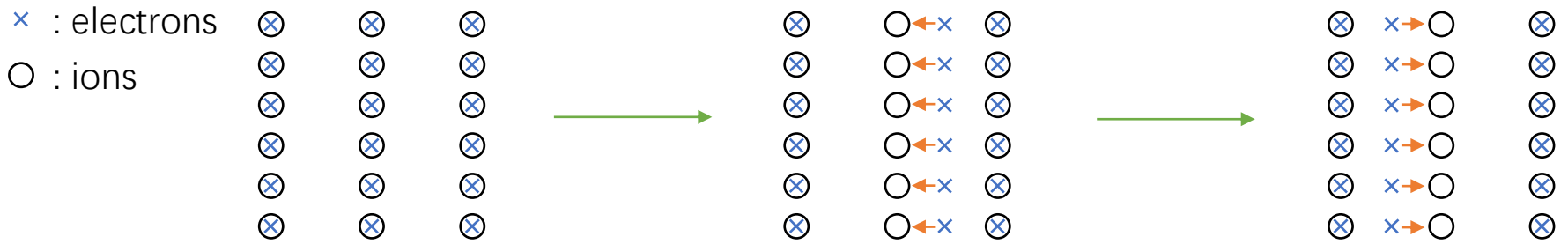

$$\nabla \cdot \vec{E} = -4\pi e n_1 \Longrightarrow eE \sim \frac{4\pi e^2 n_0}{\omega_p / v_\phi} = m\omega_p v_\phi \sim m\omega_p c$$

$$eE \sim \sqrt{\frac{n_0}{10^{18}\mathrm{cm}^{-3}}}\ \mathrm{GeV/cm}$$

$$\nabla\cdot = \frac{\partial}{\partial x} \sim ik_p$$

$$n_1 \sim n_0$$

$$k_p = \omega_p / v_\phi$$

The plasma frequency

$$\omega_p = \sqrt{\frac{4\pi e^2 n_0}{m}}$$

Challenge: A wave with $v_\phi \approx c$ is needed to accelerate light electrons!

Laser wakefield accelerator (LWFA)

- 1979, Tajima and Dawson proposed the concept of laser wakefield accelerator.

VOLUME 43, NUMBER 4 PHYSICAL REVIEW LETTERS 23 JULY 1979

Laser Electron Accelerator

T. Tajima and J. M. Dawson
Department of Physics, University of California, Los Angeles, California 90024
(Received 9 March 1979)

An intense electromagnetic pulse can create a weak of plasma oscillations through the action of the nonlinear ponderomotive force. Electrons trapped in the wake can be accelerated to high energy. Existing glass lasers of power density 10^{18}W/cm^2 shone on plasmas of densities 10^{18} cm^{-3} can yield gigaelectronvolts of electron energy per centimeter of acceleration distance. This acceleration mechanism is demonstrated through computer simulation. Applications to accelerators and pulsers are examined.

Cited by ~7000!

Laser wakefield accelerator (LWFA) and Plasma wakefield acceleration (PWFA)

- 1979, Tajima and Dawson proposed the concept of laser wakefield accelerator.

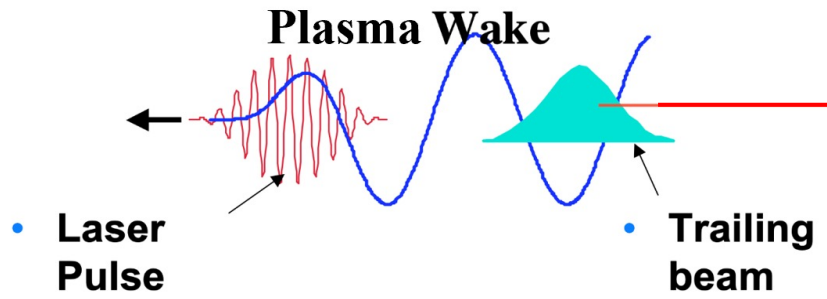

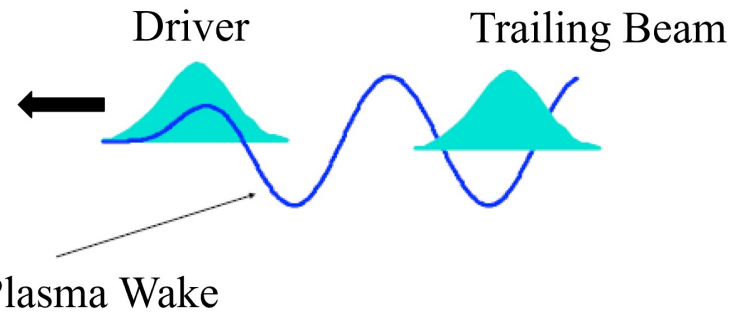

P. Chen, J. Dawson et al., *Acceleration of Electrons by the Interaction of a Bunched Electron Beam with a Plasma*, PRL 54, 693 (1985).

- Ultrashort and ultra-intense drivers: $\sim\omega_p^{-1}$ (18 fs@10^{18} cm^{-3}); $a_0=E_L/(mc/\omega_L e)$ or $\Lambda=2I/I_A\sim1$.
- Wakefield: $E_z\sim mc\omega_p/e$ (~1 GV/cm @10^{18} cm^{-3})

➢Laser-driven: Laser wakefield acceleration (LWFA)
rich laser-plasma interactions, easy to accessible

➢Beam-driven: Plasma wakefield acceleration (PWFA)
rigid, high efficiency (from wall-plug to electrons), only several facilities (SLAC, DESY, ⋯)

Laser wakefield accelerator

Wakefield excitation:
$\sim \omega_p^{-1}$

Driver evolution:
$\sim z_R$ (laser drivers) or β-function (beam drivers)

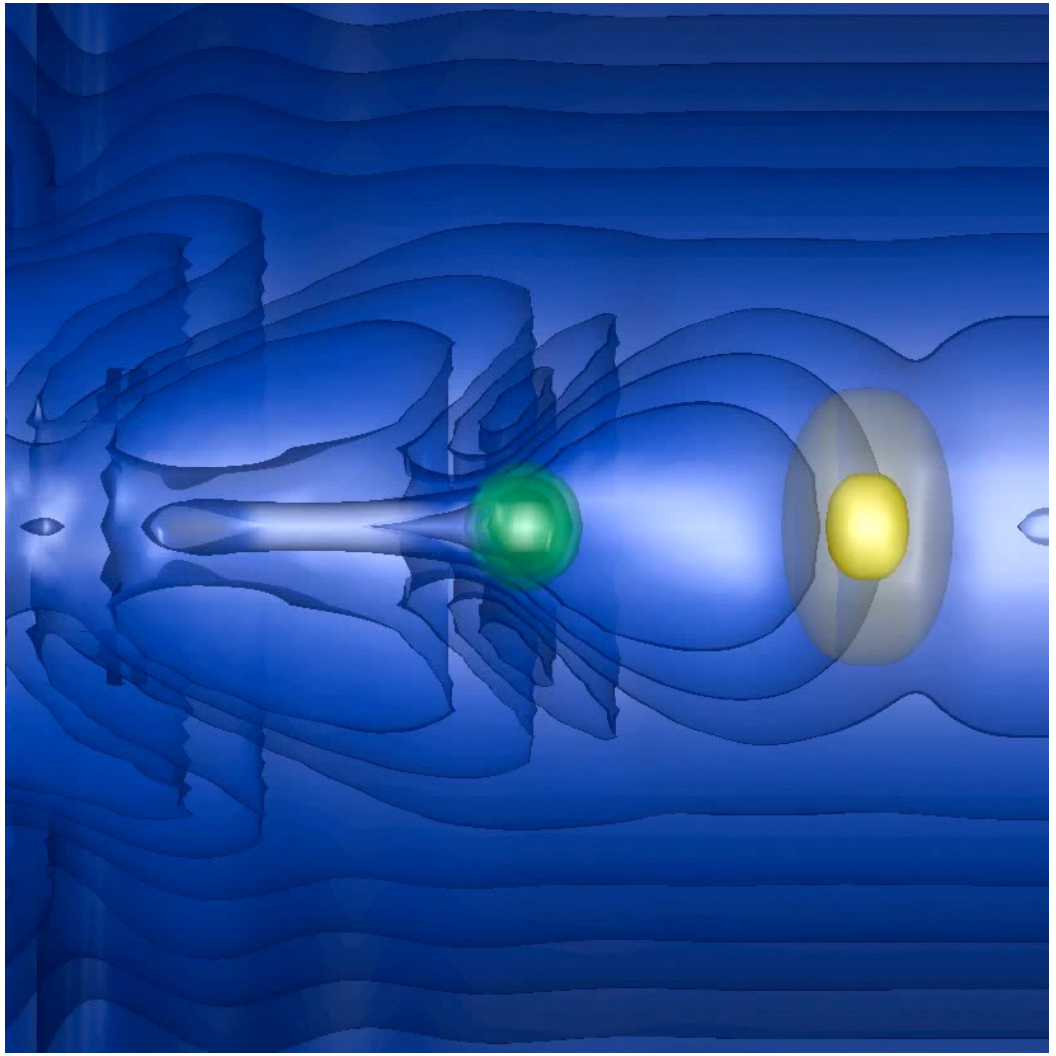

Plasma-based acceleration

- Cold, collisionless plasmas
  - ➢Dimensions: 1D, 2D, and 3D
  - ➢Intensity of drivers: linear, nonlinear
  - ➢Driver types: laser-driven, beam-driven (e^-, e^+, proton)
- A 3D linear wake
  - ➢Section 2, T. Katsouleas *et al., Beam loading in plasma accelerators,* Particle Accelerators, 1987, 22, 81-99 (1987).
  - ➢Section II-B, E. Esarey, C. B. Schroeder, and W. P. Leemans, *Physcis of laser-driven plasma-based electron accelerators*, Reviews of Modern Physics, 81, 1229 (2009).

A 3D linear wake driven by an electron beam

- Goal: understand the plasma response to a bunch of arbitrary charge moving at approximately *c*

linear regime → linear superposition works!

understand the plasma response to a single charge moving at approximately *c*

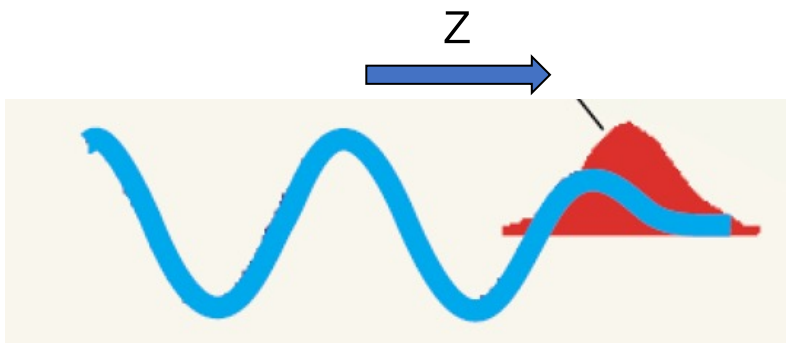

a single charge

$$\rho_0 = q\delta(\mathbf{r})\delta(z - V_b t) \quad (1)$$

A 3D linear wake: the motion Eq.

0^{th}-order quantities: n_0, $\mathbf{V}_0=0$, $\mathbf{E}_0=\mathbf{B}_0=0$
1^{st}-order quantities: q, n_1, $\mathbf{V}_1$, $\mathbf{E}_1$, $\mathbf{B}_1$

a single charge

$$\rho_0 = q\delta(\mathbf{r})\delta(z - V_b t)$$

motion eq. of plasma e^-

$$\frac{\mathrm{d}\mathbf{V}}{\mathrm{d}t} = -\frac{e}{m_e}(\mathbf{E} + \mathbf{V}\times\mathbf{B})$$

(ions don't move!)

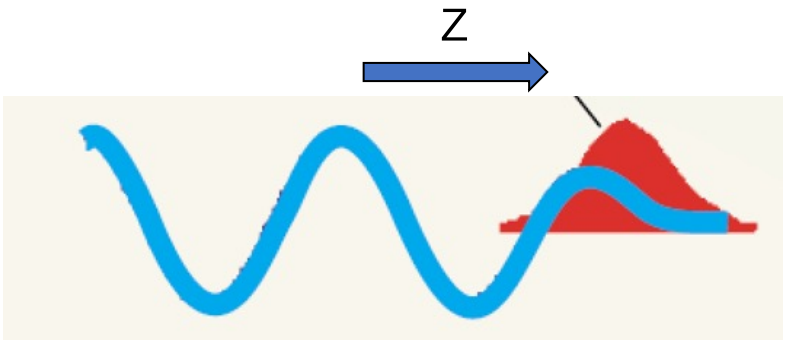

$$\frac{\mathrm{d}(\mathbf{V}_0 + \mathbf{V}_1)}{\mathrm{d}t} = -\frac{e}{m_e}[(\mathbf{E}_0 + \mathbf{E}_1) + (\mathbf{V}_0 + \mathbf{V}_1)\times(\mathbf{B}_0 + \mathbf{B}_1)]$$

$\mathbf{V}_0=0$, $\mathbf{E}_0=\mathbf{B}_0=0$

$$\frac{\mathrm{d}\mathbf{V}_1}{\mathrm{d}t} = -\frac{e}{m_e}\mathbf{E}_1$$

$$\frac{\partial\mathbf{V}_1}{\partial t} + \cancel{(\mathbf{V}_1\cdot\nabla)\mathbf{V}_1} = -\frac{e}{m_e}\mathbf{E}_1$$

A 3D linear wake: the continuity Eq.

0^{th}-order quantities: n_0, $\mathbf{V}_0=0$, $\mathbf{E}_0=\mathbf{B}_0=0$

1^{st}-order quantities: q, n_1, $\mathbf{V}_1$, $\mathbf{E}_1$, $\mathbf{B}_1$

a single charge

$$\rho_0 = q\delta(\mathbf{r})\delta(z - V_b t)$$

continuity eq. of plasma e^-

$$\frac{\partial n}{\partial t} + \nabla \cdot (n\mathbf{V}) = 0$$

$$\frac{\partial (n_0 + n_1)}{\partial t} + \nabla \cdot [(n_0 + n_1)(\mathbf{V}_0 + \mathbf{V}_1)] = 0$$

$V_0=0$

$$\frac{\partial n_1}{\partial t} + \nabla \cdot (n_0 \mathbf{V}_1) = 0$$

$$\frac{\partial n_1}{\partial t} + n_0 \nabla \cdot \mathbf{V}_1 = 0$$

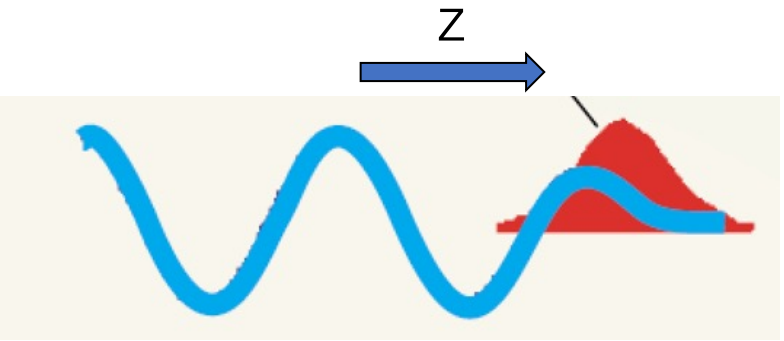

A 3D linear wake: Maxwell's Eqs.

a single charge

$$\rho_0 = q\delta(\mathbf{r})\delta(z - V_b t)$$

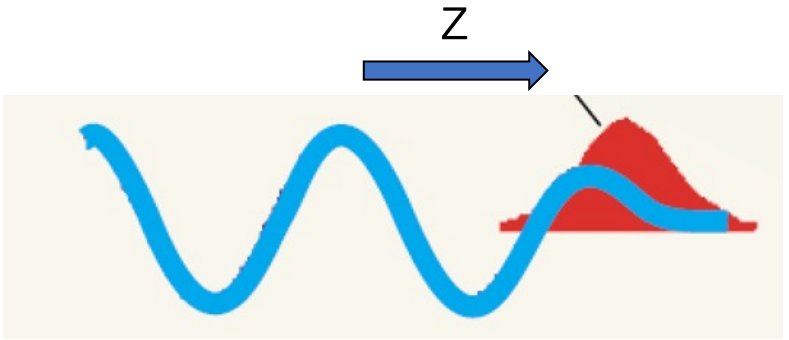

0^{th}-order quantities: n_0, $\mathbf{V}_0=0$, $\mathbf{E}_0=\mathbf{B}_0=0$

1^{st}-order quantities: q, n_1, $\mathbf{V}_1$, $\mathbf{E}_1$, $\mathbf{B}_1$

Maxwell's Eqs. $\nabla \cdot \mathbf{E} = 4\pi\rho$

$\mathbf{E}_0=0$

$$\rho = \rho_{ion} + \rho_e + \rho_0 = -en_1 + \rho_0$$

$$\nabla \cdot \mathbf{E}_1 = -4\pi e n_1 + 4\pi\rho_0$$

$$\nabla \times \mathbf{E}_1 = -\frac{1}{c}\frac{\partial \mathbf{B}_1}{\partial t}$$

$$\nabla \times \mathbf{B}_1 = \frac{4\pi}{c}\mathbf{j} + \frac{1}{c}\frac{\partial \mathbf{E}_1}{\partial t}$$

$$\nabla \cdot \mathbf{B}_1 = 0$$

Gaussian Units (cgs)

A 3D linear wake: Linearized Eqs.

a single charge

$$\rho_0 = q\delta(\mathbf{r})\delta(z - V_b t)$$

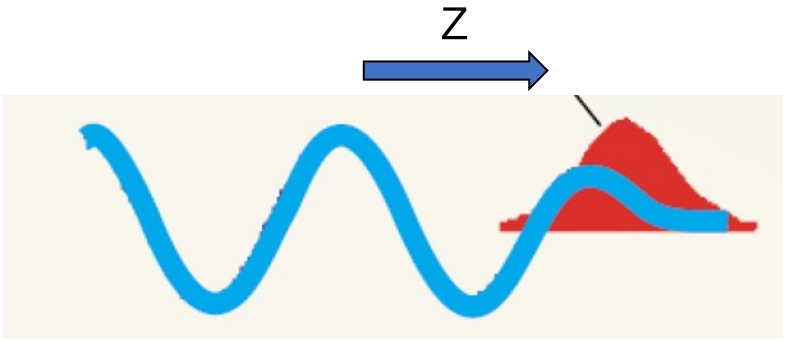

motion eq.

$$\frac{\partial \mathbf{V}}{\partial t} = -\frac{e}{m_e}\mathbf{E} \tag{2}$$

continuity eq.

$$\frac{\partial n_1}{\partial t} + n_0 \nabla \cdot \mathbf{V} = 0 \tag{3}$$

Maxwell's eqs.

$$\nabla \cdot \mathbf{E} = -4\pi e n_1 + 4\pi\rho_0 \tag{4}$$

$$\nabla \times \mathbf{E} = -\frac{1}{c}\frac{\partial \mathbf{B}}{\partial t} \tag{5}$$

$$\nabla \times \mathbf{B} = \frac{4\pi}{c}\mathbf{j} + \frac{1}{c}\frac{\partial \mathbf{E}}{\partial t} \tag{6}$$

$$\nabla \cdot \mathbf{B} = 0$$

The response of the plasma density: n_1

Taking the first derivative of (3) and substituting from (2) gives

$$\frac{\partial^2 n_1}{\partial t^2} + n_0 \nabla \cdot (-e\mathbf{E}/m_e) = 0$$

Substituting for ∇·E from (4) gives the wave equation for the plasma response

$$\nabla \cdot \mathbf{E} = -4\pi e n_1 + 4\pi \rho_0$$

$$\left(\frac{\partial^2}{\partial t^2} + \omega_p^2\right) n_1 = \omega_p^2 \frac{\rho_0}{e} = \omega_p^2 \frac{q}{e} \delta(\mathbf{r}) \delta\left(t - \frac{z}{V_b}\right) \frac{1}{V_b}$$

Green's function for a harmonic oscillator

plasma frequency $\omega_p = \sqrt{\frac{4\pi e^2 n_0}{m_e}}$

$$n_1 = \frac{\omega_p q \delta(\mathbf{r})}{V_b e} \sin\left[\omega_p (t - z/V_b)\right] \theta(t - z/V_b)$$

a single charge

$$\rho_0 = q\delta(\mathbf{r})\delta(z - V_b t)$$

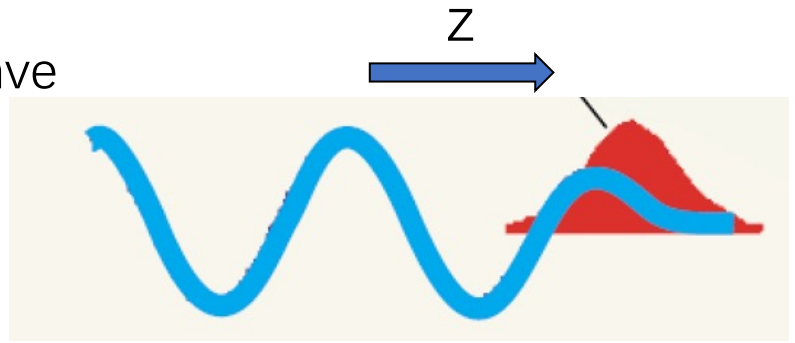

There are different approaches to get the solution.

Wakefields: E and B

Taking the curl of (5) and substituting the time derivative of (6)

$$\left(\frac{\partial^2}{\partial t^2} - c^2\nabla^2\right)\mathbf{E} = -4\pi\frac{\partial \mathbf{j}}{\partial t} - c^2\nabla(\nabla\cdot\mathbf{E})$$

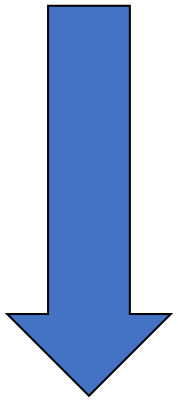

$$\frac{\partial \mathbf{j}_p}{\partial t} = -n_0 e\frac{\partial \mathbf{V}}{\partial t} = n_0 e^2\frac{\mathbf{E}}{m_e}$$

From (2)

$$\mathbf{j}_0 = q\rho_0 V_b \hat{z}$$

$$\nabla\cdot\mathbf{E} = -4\pi e n_1 + 4\pi\rho_0$$

A relation between current and E-field is important for the wave equation.

$$\left[\frac{\partial^2}{\partial t^2} - c^2\left(\nabla_\perp^2 + \frac{\partial^2}{\partial z^2}\right) + \omega_p^2\right]\mathbf{E} = -4\pi\frac{\partial \mathbf{j}_0}{\partial t} + 4\pi c^2\nabla\left(e n_1 - \rho_0\right)$$

$$\left[\frac{\partial^2}{\partial t^2} - c^2\left(\nabla_\perp^2 + \frac{\partial^2}{\partial z^2}\right) + \omega_p^2\right]\mathbf{B} = 4\pi c\nabla\times\mathbf{j}_0$$

Wakefields: A summary of the key eqs.

$$\begin{cases} \left(\dfrac{\partial^2}{\partial t^2} + \omega_p^2\right) n_1 = \omega_p^2 \dfrac{\rho_0}{e} \\ \left[\dfrac{\partial^2}{\partial t^2} - c^2\left(\nabla_\perp^2 + \dfrac{\partial^2}{\partial z^2}\right) + \omega_p^2\right] \mathbf{E} = -4\pi \dfrac{\partial \mathbf{j}_0}{\partial t} + 4\pi c^2 \nabla \left(e n_1 - \rho_0\right) \\ \left[\dfrac{\partial^2}{\partial t^2} - c^2\left(\nabla_\perp^2 + \dfrac{\partial^2}{\partial z^2}\right) + \omega_p^2\right] \mathbf{B} = 4\pi c \nabla \times \mathbf{j}_0 \end{cases}$$

wave operator

$$\mathbf{j}_0 = \rho_0 V_b \hat{z}$$

Quasi-static approximation (QSA)

Old coordinates: z, t

New coordinates: $\xi \equiv z - V_b t$, $\tau = t$

Galilean transformation

ξ: axial position in the moving frame
τ: the propagation time (distance)

$$\begin{cases} \dfrac{\partial}{\partial t} = \dfrac{\partial}{\partial \tau}\dfrac{\partial \tau}{\partial t} + \dfrac{\partial}{\partial \xi}\dfrac{\partial \xi}{\partial t} \\ \qquad\quad = \dfrac{\partial}{\partial \tau} - V_b \dfrac{\partial}{\partial \xi} \\ \dfrac{\partial}{\partial z} = \dfrac{\partial}{\partial \tau}\dfrac{\partial \tau}{\partial z} + \dfrac{\partial}{\partial \xi}\dfrac{\partial \xi}{\partial z} \\ \qquad\quad = \dfrac{\partial}{\partial \xi} \end{cases}$$

Quasi-static approximation

$$\left|\frac{\partial}{\partial \tau}\right| \ll \left|V_b \frac{\partial}{\partial \xi}\right|$$

$$\frac{\partial^2}{\partial t^2} - c^2 \frac{\partial^2}{\partial z^2} \approx (V_b^2 - c^2)\frac{\partial^2}{\partial \xi^2} \approx 0$$

$V_b \approx c$

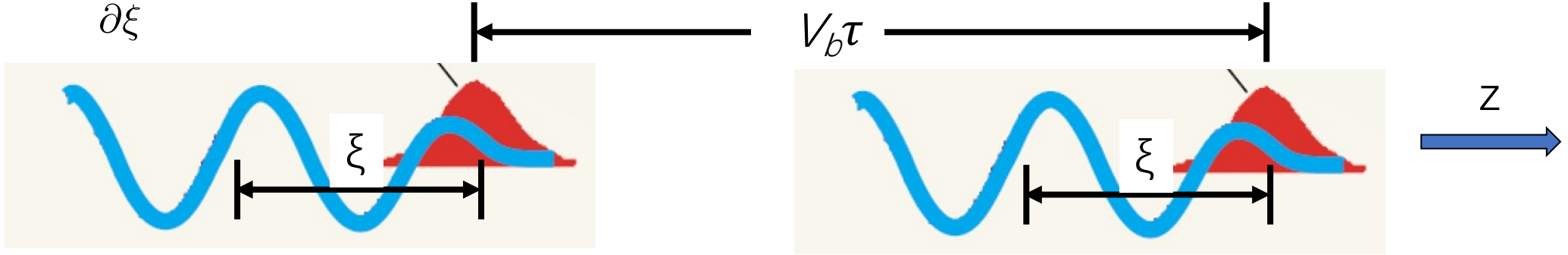

Wakefields: E and B

$$\left[\frac{\partial^2}{\partial t^2} - c^2\left(\nabla_\perp^2 + \frac{\partial^2}{\partial z^2}\right) + \omega_p^2\right]\mathbf{E} = -4\pi\frac{\partial \mathbf{j}_0}{\partial t} + 4\pi c^2 \nabla\left(en_1 - \rho_0\right)$$

QSA

$$\left(\nabla_\perp^2 - k_p^2\right)\mathbf{E} = -4\pi e\nabla n_1 + 4\pi\left(\frac{1}{c^2}\frac{\partial \mathbf{j}_0}{\partial t} + \nabla\rho_0\right)$$

$$\left(\frac{\partial^2}{\partial t^2} + \omega_p^2\right) n_1 = \omega_p^2\frac{\rho_0}{e}$$

$$n_1 = \frac{\omega_p q\delta(\mathbf{r})}{V_b e}\sin\left[\omega_p(t - z/V_b)\right]\theta(t - z/V_b)$$

- For the longitudinal wake field E_z,

$$\left(\nabla_\perp^2 - k_p^2\right)E_z = -\frac{4\pi\omega_p q}{c}\frac{\partial}{\partial z}\left[\delta(\mathbf{r})\theta(t - z/c)\sin\left[\omega_p(t - z/c)\right]\right]$$

The radial dependence of E_z is simply the Green's function response to the Kelvin-Helmholtz equation.

$$E_z = -2qk_p^2 K_0(k_p r)\theta(t - z/c)\cos\left[\omega_p(t - z/c)\right]$$

Wakefields: E and B

$$W_{\parallel,\perp} = \left(\mathbf{E} + \frac{\mathbf{V}\times\mathbf{B}}{c}\right)_{z,r}$$

- We use **the Panofsky-Wenzel theorem** to get the transverse wakefield, $\frac{\partial W_\parallel}{\partial r} = \frac{\partial W_\perp}{\partial z}$

$$\frac{\mathrm{d}}{\mathrm{d}x}K_0(x) = -K_1(x)$$

$$W_\perp = (E_r - B_\theta) = \int \mathrm{d}z \frac{\partial W_\parallel}{\partial r}$$

$$= -2qk_p^2 K_1(k_p r)\theta(t - z/c)\sin\left[\omega_p(t - z/c)\right]$$

- B fields are 2nd-order quantities in a linear wake

$$\left[\frac{\partial^2}{\partial t^2} - c^2\left(\nabla_\perp^2 + \frac{\partial^2}{\partial z^2}\right) + \omega_p^2\right]\mathbf{B} = 4\pi c\nabla\times\mathbf{j}_0 \quad \Rightarrow \quad \left(\nabla_\perp^2 - k_p^2\right)\mathbf{B} = -\frac{4\pi}{c}\nabla\times\mathbf{j}_0$$

It is the B-field of a beam driver if k_p^2 term is neglected.

Wakefields excited by an electron beam

- General expression:

$$E_z(r,\theta,\xi) = (-2k_p^2)\int_{+\infty}^{\xi} \mathrm{d}\xi' \int_0^{\infty} r'\mathrm{d}r' \int_0^{2\pi} \mathrm{d}\theta' \rho_b(r',\theta',\xi') \times K_0(k_p|\mathbf{r}-\mathbf{r}'|)\cos\left[k_p(\xi-\xi')\right]$$

- If the charge density ρ_b is separable, then

$$\rho_b = \rho_{\parallel} \cdot \rho_{\perp}(r,\theta)$$

$$W_{\parallel} = E_z(r,\xi) = Z'(\xi)R(r)$$

$$W_{\perp} = E_r(r,\xi) - B_\theta(r,\xi) = Z(\xi)R'(r)$$

where $Z'(\xi) = -4\pi \int_{+\infty}^{\xi} \mathrm{d}\xi' \rho_{\parallel}(\xi')\cos\left[k_p(\xi-\xi')\right]$

$$R(r) = \frac{k_p^2}{2\pi}\int_0^{2\pi} \mathrm{d}\theta \int_0^{+\infty} r'\mathrm{d}r' \rho_{\perp}(r',\theta) K_0(k_p|\mathbf{r}-\mathbf{r}'|)$$

Wakefields excited by an electron beam

- If the driver is axial symmetric, $\rho_b = \rho_{\parallel} \cdot \rho_{\perp}(r,\theta) = \rho_{\parallel} \cdot \rho_r(r)$

$$Z'(\xi) = -4\pi \int_{+\infty}^{\xi} \mathrm{d}\xi' \rho_{\parallel}(\xi') \cos\left[k_p(\xi - \xi')\right]$$ sinusoidal oscillation behind the driver

$$R(r) = \frac{k_p^2}{2\pi} \int_0^{2\pi} \mathrm{d}\theta \int_0^{+\infty} r' \mathrm{d}r' \rho_{\perp}(r',\theta) K_0(k_p|\mathbf{r} - \mathbf{r}'|)$$

$$K_0(k_p|\mathbf{r} - \mathbf{r}'|) = I_0(k_p r_<) K_0(k_p r_>) + 2\sum_{m=1}^{+\infty} \cos m\theta I_m(k_p r_<) K_m(k_p r_>)$$

$r_<$, $r_>$ are the larger or smaller of r and r'

$$R(r) = k_p^2 \int_0^{+\infty} r' \mathrm{d}r' \rho_r(r') I_0(k_p r_<) K_0(k_p r_>)$$

➢ Example: a flat top profile with radius a

$$R(r) = \begin{cases} 1 - k_p a K_1(k_p a) I_0(k_p r) & r < a \\ k_p a I_1(k_p a) K_0(k_p r) & r > a \end{cases}$$

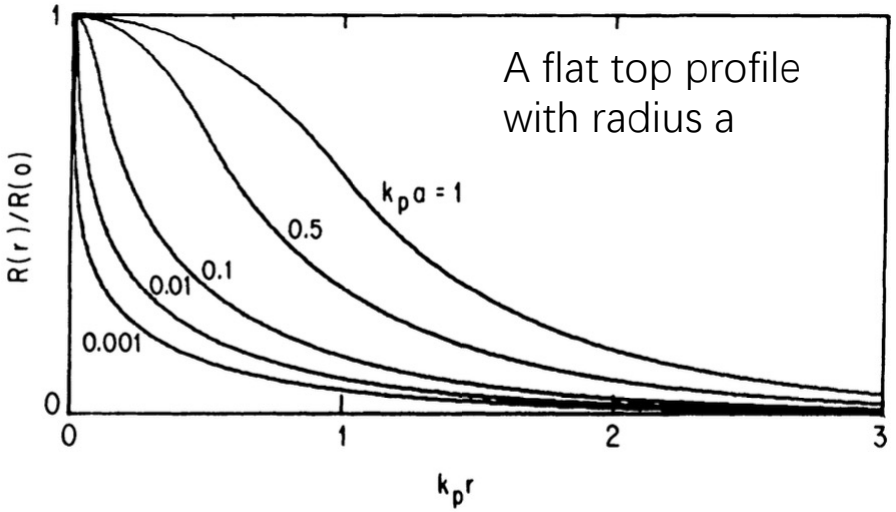

Wakefields excited by an electron beam

- Narrow beams: $k_p\sigma_r<<1$
  - (1) For a tightly focused beam ($k_p\sigma_r<<1$), wakefield is relatively insensitive both to shape and size of the beam;
  - (2) Even if the beam is much narrower than c/ω_p, the effect of the beam is felt out to a c/ω_p;
  - (3) For an accelerating beam, energy of the wake out to c/ω_p will be absorbed by the beam.
- Wide beams: $k_p\sigma_r>>1$

$$R(r) \sim \rho_r(r)$$

$$\left(\nabla_\perp^2 - k_p^2\right)\mathbf{E} = -4\pi e\nabla n_1 + 4\pi\left(\frac{1}{c^2}\frac{\partial \mathbf{j}_0}{\partial t} + \nabla\rho_0\right)$$

Pseudo-potential ψ

- Scala potential ϕ and vector potential **A**

$$\left(\frac{1}{c^2}\frac{\partial^2}{\partial t^2}-\nabla^2\right)\mathbf{A}=4\pi\frac{\mathbf{j}}{c}$$

$$\left(\frac{1}{c^2}\frac{\partial^2}{\partial t^2}-\nabla^2\right)\phi=4\pi\rho$$

Lorenz gauge

$$\nabla\cdot\mathbf{A}+\frac{1}{c}\frac{\partial\phi}{\partial t}=0$$

- Quasi-static approximation: ψ = ϕ - A_z

$$-\nabla_\perp^2\psi=4\pi\left(\rho-j_z/c\right)$$

$$\mathbf{E}=-\nabla\phi-\frac{1}{c}\frac{\partial\mathbf{A}}{\partial t}$$

$$\mathbf{B}=\nabla\times\mathbf{A}$$

QSA

$$E_z=-\frac{\partial\psi}{\partial\xi}$$

$$B_z=\left(\nabla_\perp\times\mathbf{A}_\perp\right)\cdot\hat{z}$$

A representation of the Panofsky-Wenzel theorem

$$\mathbf{E}_\perp+c\hat{z}\times\mathbf{B}_\perp=-\nabla_\perp\psi$$

$$\begin{cases}\mathbf{E}_\perp=-\nabla_\perp\phi-\dfrac{\partial\mathbf{A}_\perp}{\partial\xi}\\ \mathbf{B}_\perp=\nabla_\perp\times\left(A_z\hat{z}\right)+\nabla_z\times\mathbf{A}_\perp\end{cases}$$

Pseudo-potential ψ

- The equation of ψ in a 3D linear wake (under QSA)

$$\left(\nabla_\perp^2 - k_p^2\right) E_z = -4\pi e \frac{\partial}{\partial z} n_1$$

$$E_z = -\frac{\partial \psi}{\partial \xi}$$

$$\left(\nabla_\perp^2 - k_p^2\right) \psi = 4\pi e n_1$$

or $\quad -\nabla_\perp^2 \psi = 4\pi \left(\rho - j_z/c\right)$

- The solution is $\psi(r,\xi) = R(r)Z(\xi)$
- In the wide beam limit: $\psi(r,\xi) \approx -\dfrac{m_e c^2}{e} \dfrac{n_1(r,\xi)}{n_0}$

A linear wake driven by a laser pulse

E and **B** doesn't contain laser fields.

$$m_e \frac{\mathrm{d}\mathbf{V}}{\mathrm{d}t} = -e\left(\mathbf{E} + \mathbf{V} \times \mathbf{B}\right) + \mathbf{F}_p$$

$$\left(\frac{\partial^2}{\partial t^2} + \omega_p^2\right) n_1 = \omega_p^2 \frac{\rho_0}{e} + \frac{\omega_p^2}{4\pi e^2} \nabla^2 \phi_p$$

$$\left(\nabla_\perp^2 - k_p^2\right) \psi = 4\pi e n_1 - \frac{k_p^2}{e} \phi_p$$

$$\left(\nabla_\perp^2 - k_p^2\right) \left(\frac{\partial^2}{\partial \xi^2} + k_p^2\right) \psi = 4\pi k_p^2 \rho_0 + \frac{k_p^2}{e} \left(\nabla_\perp^2 - k_p^2\right) \phi_p$$

Pondermotive force Approximation

F_p - pondermotive force

ϕ_p - pondermotive potential

Ref.: Section II and Appendix A&B, P. Mora and J. Antonsen, *Kinetic modeling of intense, short laser pulses propagating in tenuous plasmas,* Phys. Plasmas, 4, 217 (1997).

A linear wake driven by a laser pulse

$$\left(\nabla_\perp^2 - k_p^2\right)\left(\frac{\partial^2}{\partial\xi^2} + k_p^2\right)\psi = 4\pi k_p^2\rho_0 + \frac{k_p^2}{e}\left(\nabla_\perp^2 - k_p^2\right)\phi_p$$

Laser driver only

$$\left(\frac{\partial^2}{\partial\xi^2} + k_p^2\right)\psi = \frac{k_p^2}{e}\phi_p$$

- The transverse distribution of the acceleration field [R(r)] is the same as the laser transverse distribution.

$$\psi(r,\xi) = R(r)Z(\xi)$$

$$W_\parallel = E_z(r,\xi) = Z'(\xi)R(r)$$

$$W_\perp = E_r(r,\xi) - B_\theta(r,\xi) = Z(\xi)R'(r)$$

$$\phi_p = m_e c^2 a^2/4$$

$$a = \frac{e}{m_e c}A$$

normalized vector potential

An example of a linear wake

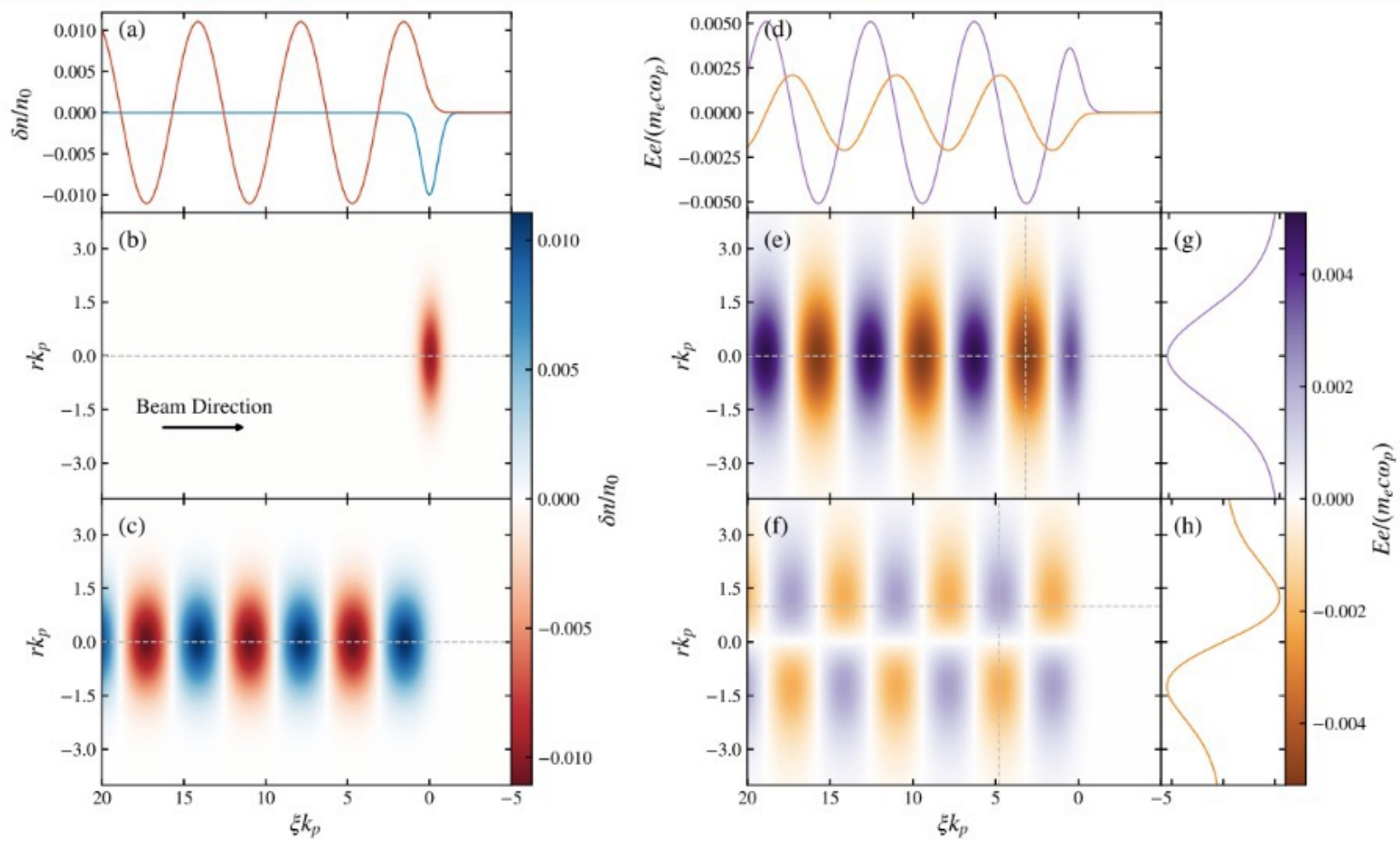

(1) $W_{//}$ is 90 out of phase with $W_{\perp}$: there is a quarter wake period that is both accelerating and focusing for e^- and e^+.

(2) $W_{//}$ has r-dependence: not ideal for uniform acceleration of beam.

(3) $W_{\perp}$ has nonlinear dependence on r: not ideal for beam emittance preservation.


We want higher fields!
From linear to nonlinear.

From linear to nonlinear

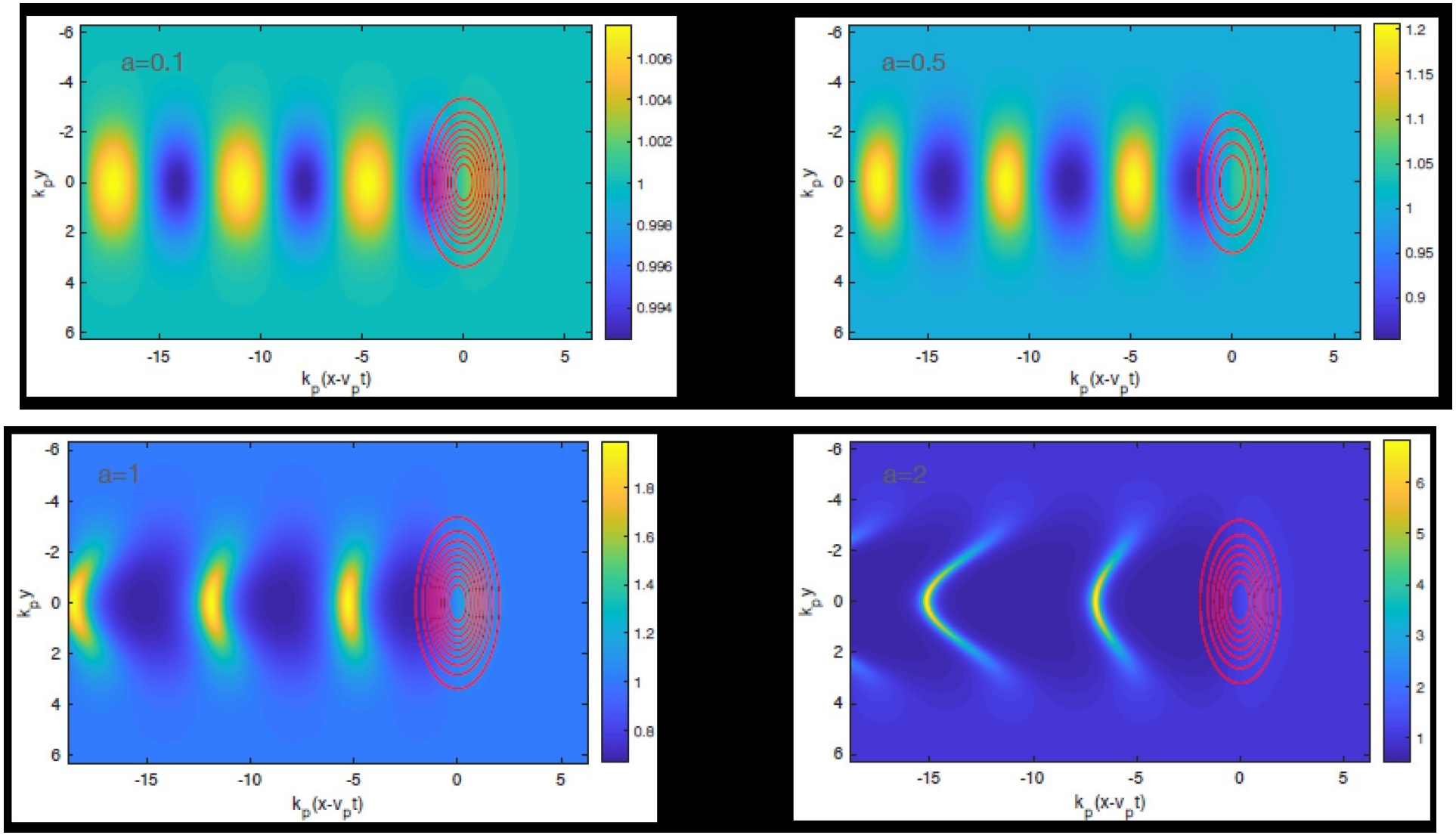

Bubble/Blowout/Fully nonlinear Regime

- Laser-driven: 1991, W. Mori *et al.,* Proceedings of the PAC, San Francisco, CA.
- Beam-driven: 1991, J. Rosenzweig *et al.,* PRA, 44, R6189.

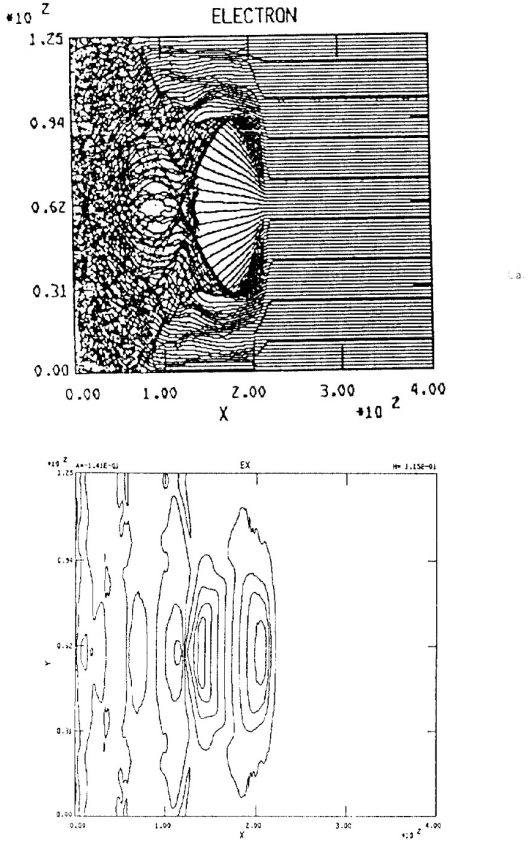

Figure 1: a) The x-y phase space of the plasma electrons. b) The accelerating electric field.

It happens in multi-dimensional geometry when the driver is intense.

- A wake devoid of plasma electrons
- Linear focusing force
- Transversely uniform acceleration field

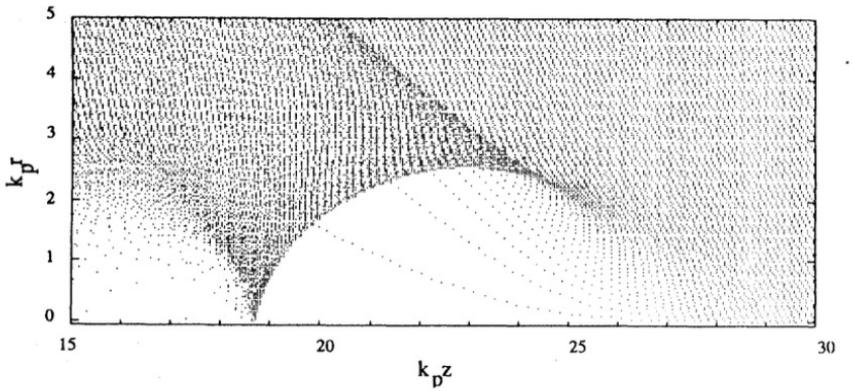

FIG. 1. Plot of plasma-electron positions from a PIC simulation of wake fields with $n_b/n_0=4$, $k_p\sigma_z=1.8$, and $k_p\sigma_r=0.6$ at the point where the beam center $k_p\xi_0=25.5$. Note that for the first oscillation a rarefied cavity forms, and that the motion is nearly laminar. After the first oscillation the wave breaks and the motion becomes very nonlaminar. Beam travels to right in this simulation.

Bubble/Blowout/Fully nonlinear Regime

- Phenomenological models

- I. Kostyukov, A. Pukhov, S. Kiselev, *Phenomenological theory of laser-plasma interaction in "bubble" regime*, Phys. Plasmas 11, 5256–5264 (2004)
- W. Lu et al., *Nonlinear Theory for Relativistic Plasma Wakefields in the Blowout Regime*, PRL 96, 165002 (2006)
- A. Golovanov et al., *Energy-Conserving Theory of the Blowout Regime of Plasma Wakefield*, PRL 130, 105001 (2023)

Bubble/Blowout/Fully nonlinear Regime

Driven by an electron beam

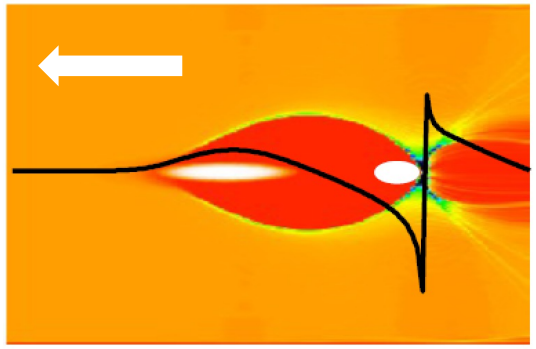

Driven by a laser pulse

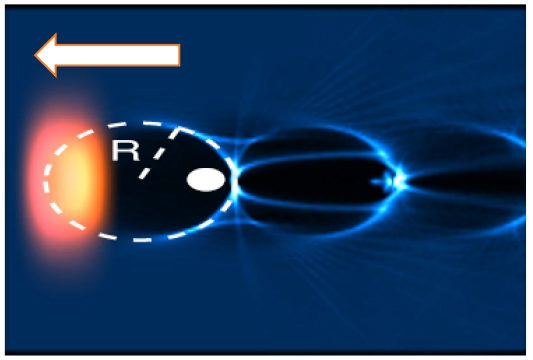

- Lineally focusing field $\hat{W}_\perp = \dfrac{\hat{r}}{2}$
- Accelerating field is uniform along r-direction

$$\frac{\partial W_\parallel}{\partial r} = \frac{\partial W_\perp}{\partial z}$$

- **Almost** ideal for high-quality beam acceleration
- Acceleration field changes longitudinally $\dfrac{\partial \hat{W}_\perp}{\partial \hat{\xi}} \approx \dfrac{1}{2}$

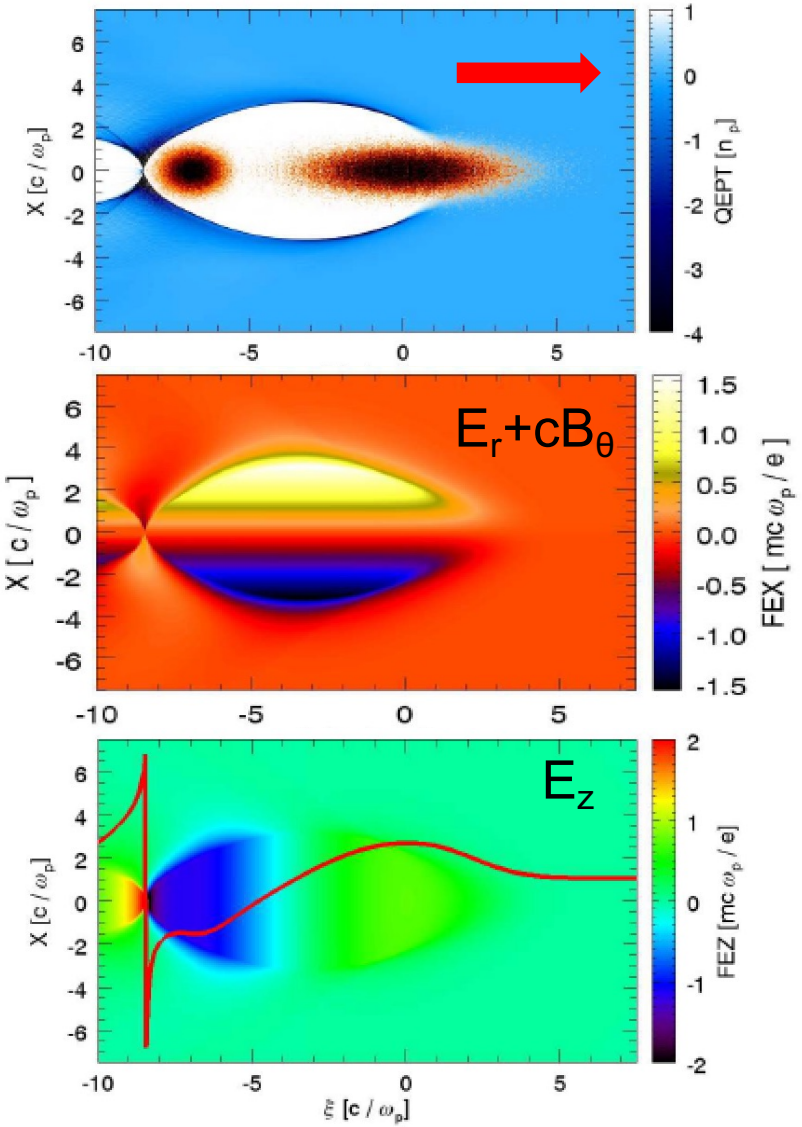

Beam Loading

- The witness/accelerated beam modifies the field distribution.
- Goal: modify the acceleration field to make it uniform across the witness beam

➢Linear regime (1D, 2D, 3D): straightforward since the linear superposition is satisfied. T. Katsouleas *et al., Beam loading in plasma accelerators,* Particle Accelerators, 1987, 22, 81-99 (1987).

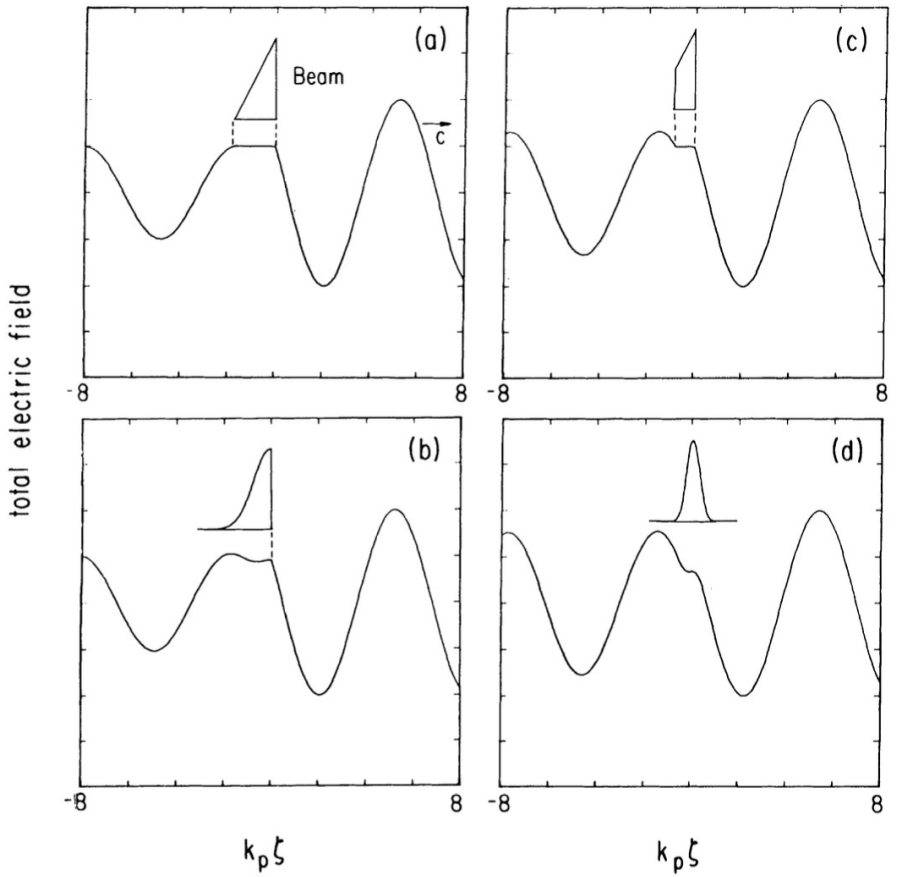

FIGURE 4 Total electric field for various beam shapes: (a) triangle [Eq. (22), $N = 3N_0/4$, $k_p\zeta_0 = \pi/3$), (b) half-Gaussian of same number of particles, (c) truncated triangle ($N = 9N_0/16$), and (d) Gaussian of same number as (c).

Beam Loading

- Goal: modify the acceleration field to make it uniform across the witness beam

➢1D nonlinear regime: J. Rosenzweig, *Nonlinear Plasma Dynamics in the Plasma Wave-Field Accelerator,* PRL 58, 555 (1987).

➢Blowout regime: M. Tzoufras *et al.*, *Beam loading in the Nonlinear Regime of Plasma-Based Acceleration*, PRL 101, 145002 (2008).

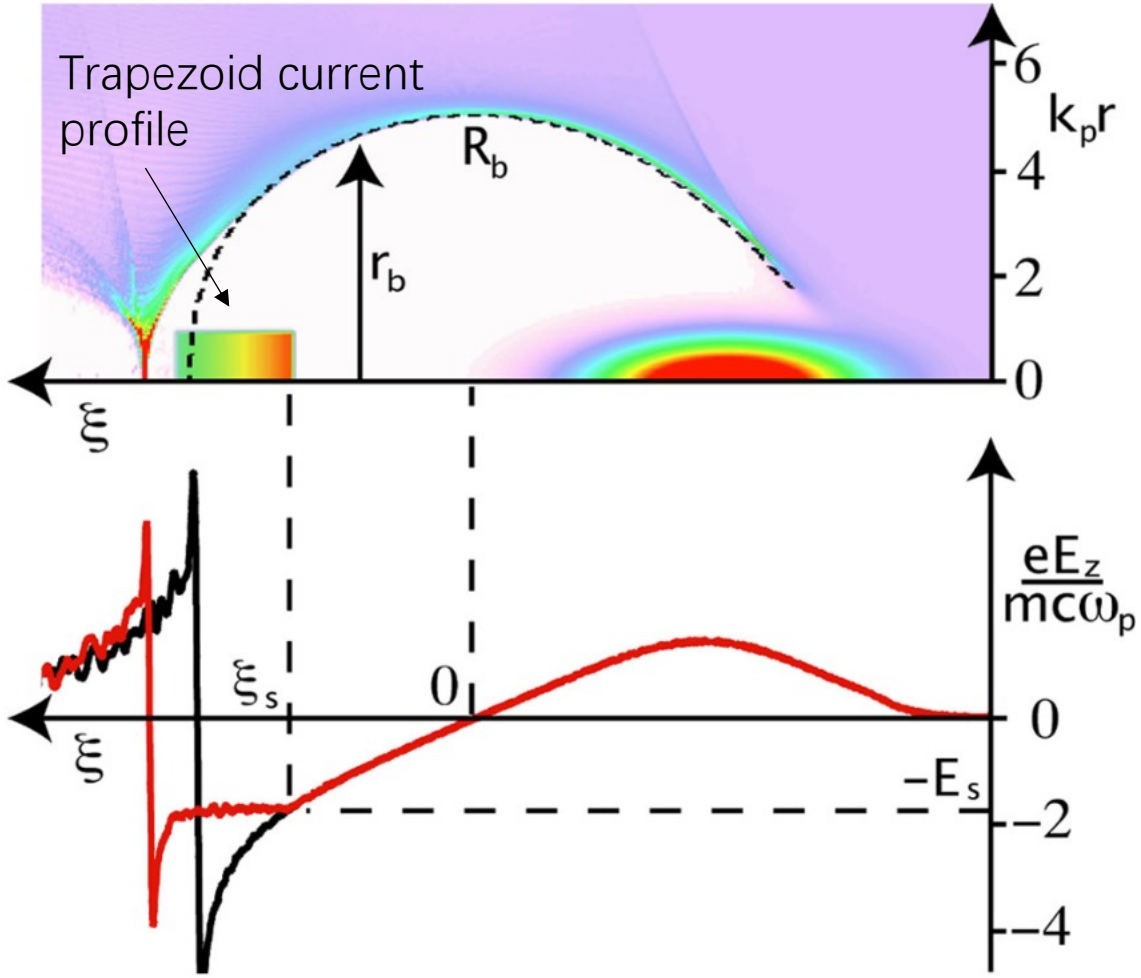

Long distance acceleration: limitations

Electrostatic acceleration

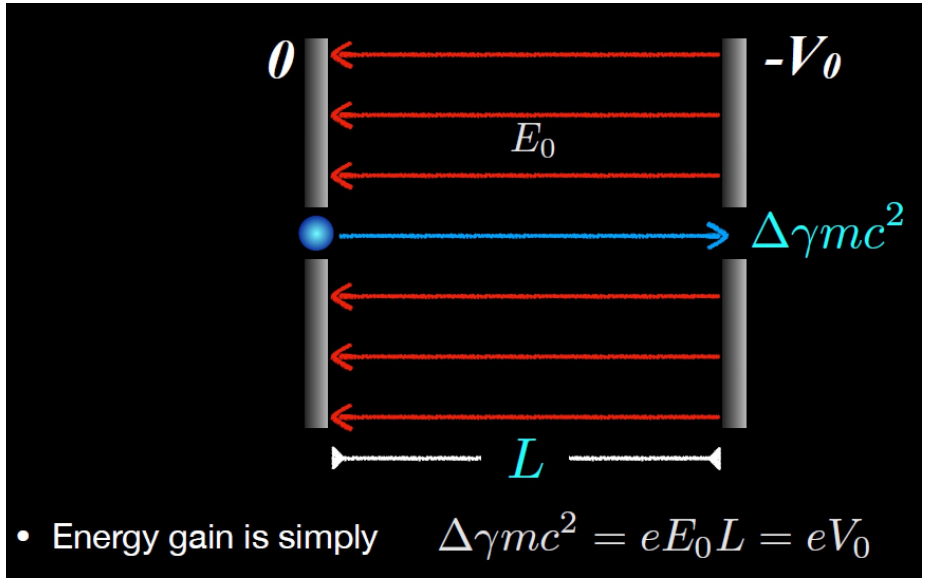

Wakefield acceleration

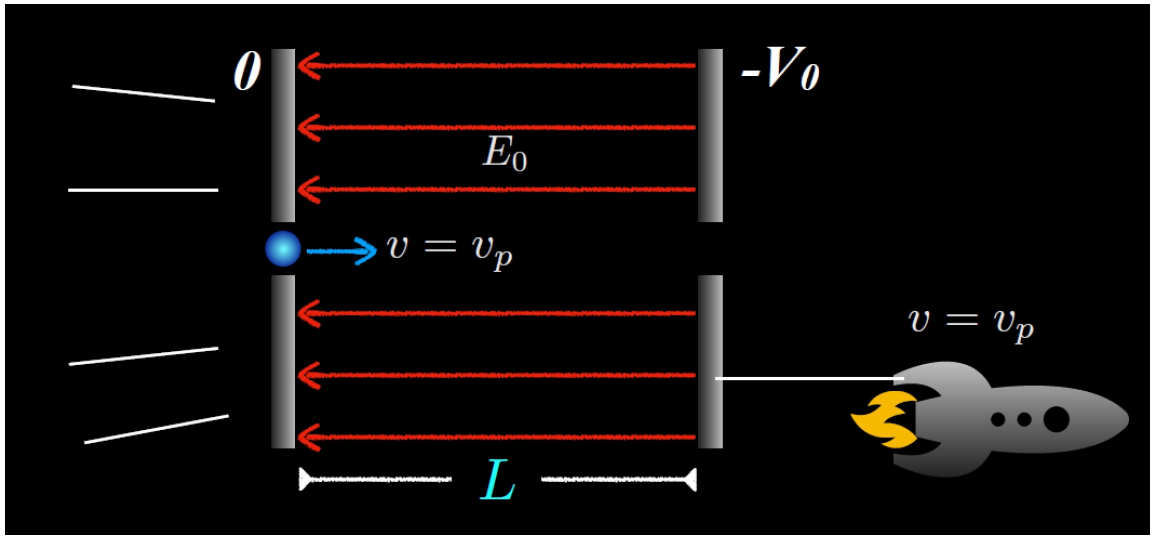

Long distance acceleration: limitations

- it reaches the end of the parallel plate - **"dephasing"**

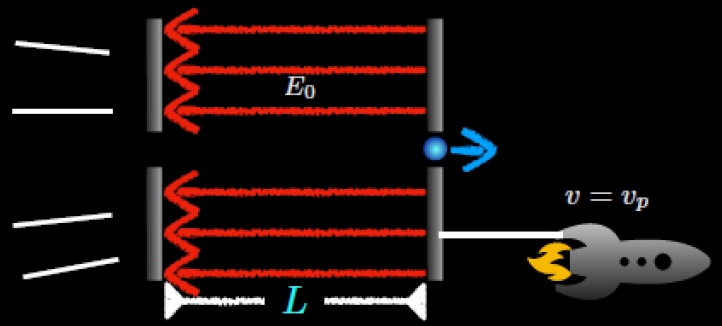

Usually limits LWFAs

- the driver runs out of energy - **"depletion"**

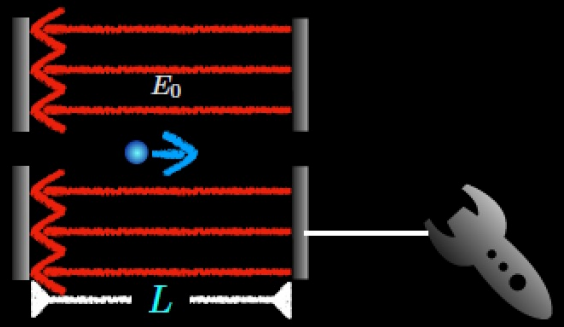

Usually limits PWFAs

Long distance acceleration

- Dephasing: $v_{\phi,wake} = v_{g,laser} = c\sqrt{1 - \frac{\omega_p^2}{\omega_0^2}} < c \quad \left(\gamma_{\phi,wake} = \frac{\omega_0}{\omega_p} = \sqrt{\frac{n_c}{n_p}} = 10 \sim 100\right)$
- Diffraction: Rayleigh length ~0.4 mm@10 μm spot size and 800 nm wavelength
- Depletion: the driver gives its energy to the plasma wake

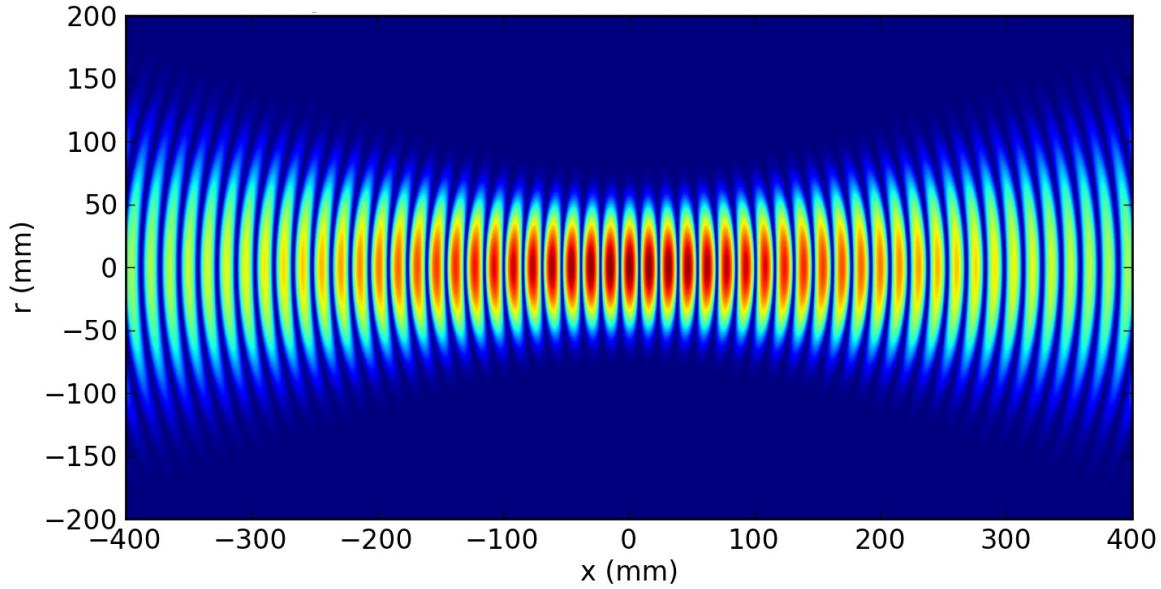

Rayleigh length

$$z_R = \frac{\pi w_0^2}{\lambda_0}$$

Long distance acceleration: Dephasing

- Dephasing: operate at low plasma density with high power lasers!

$$(c - v_{\phi,wake})\frac{L_d}{c} \approx R_b$$

$$L_d \approx R_b \frac{c}{c - v_{\phi,wake}}$$

$$v_{\phi,wake} = v_{g,laser} = c\sqrt{1 - \frac{\omega_p^2}{\omega_0^2}}$$

$$\approx 2R_b \frac{\omega_0^2}{\omega_p^2} = 2R_b \frac{n_c}{n_p}$$

$$\Delta E_{gain} \sim eL_d E_z \propto R_b \frac{n_c}{n_p}\frac{mc\omega_p}{e} \propto \frac{n_c}{n_p}$$

Beam drivers: $L_{dep} \approx 2\gamma_d^2 R_b$

$$v_{\phi,wake} = v_{g,beam} = c\sqrt{1 - \frac{1}{\gamma_d^2}}$$

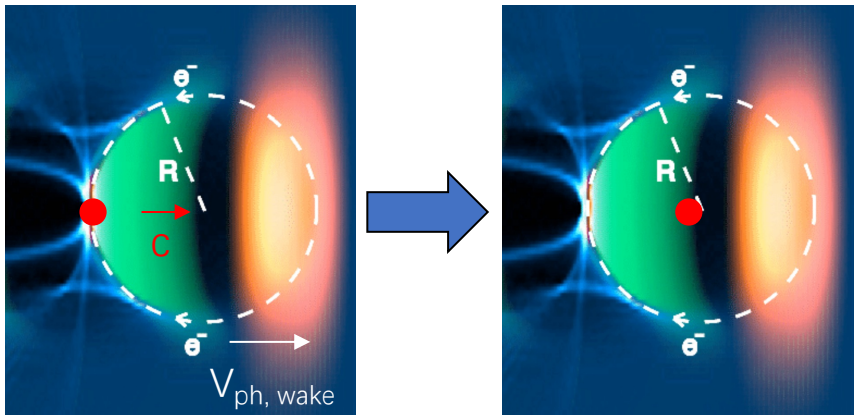

Example：

(1) n_p=10^{19} cm^{-3}, a_0=4, R_b=6.7 μm,
L_{dep}=2.3 mm, E_z~ mcω_p/e=3 GV/m

(2) n_p=10^{17} cm^{-3}, a_0=4, R_b=67 μm,
L_{dep}=2.3×10×10^2 mm, E_z~ mcω_p/e=0.3 GV/m

Long distance acceleration: Guiding

- Diffraction: guiding

$$\eta \approx 1 - \frac{1}{2}\left(1 + \frac{\Delta n_c}{n_p}\frac{r^2}{w_0^2} + \frac{\Delta n}{n_p} - \frac{a_0^2}{8}\right)$$

external guiding self-guiding

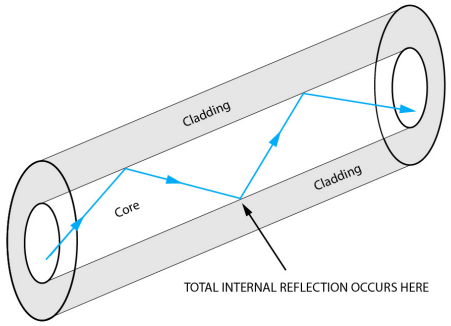

A light pulse can be guided with a nearly constant (matched) spot size by a plasma channel that has a parabolic refractive index profile with a maximum on axis.

$$\Delta n_c = \frac{1}{\pi r_e w_0^2}, \frac{\Delta n_c}{n_p} = \frac{4}{(k_p w_0)^2}$$

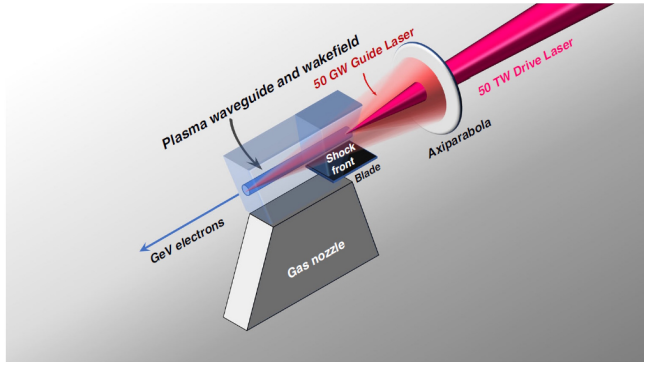

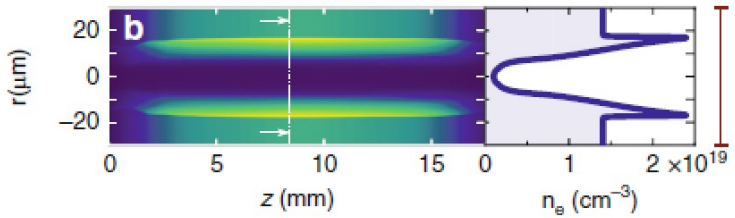

Kosta Oubrerie et al., *Controlled acceleration of GeV electron beams in an all-optical plasma waveguide*, LSA 11, 180 (2022).

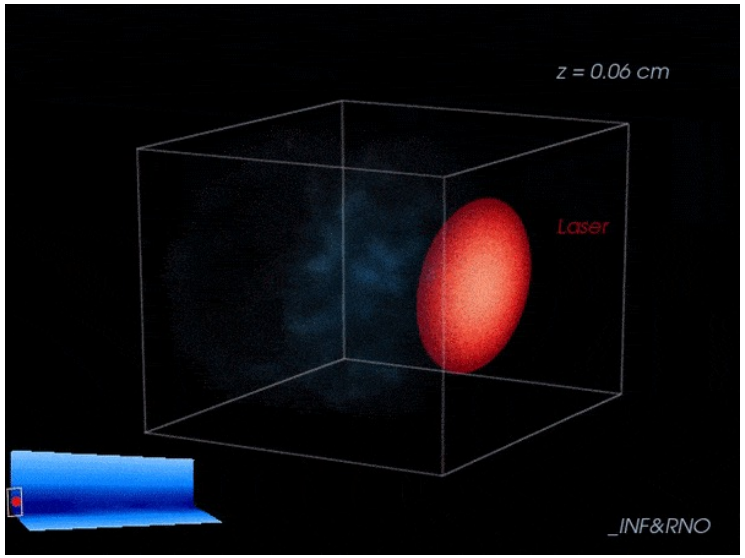

Long distance acceleration: Guiding

- How to generate the plasma channel/waveguide?

➢ Discharge capillary: LBNL, relies on the temperature profile

➢ Ignitor-Heater: A sub-ps low energy but intense 'ignitor' pulse followed by a long (10s to 100s of ps), energetic (~100 mJ) 'heater' pulse.
Ref.: P. Volfbeyn et al., *Guiding of laser pulses in plasma channels created by the ignitor-heater technique*, Phys. Plasmas 6, 2269 (1999).

➢ Bessel laser beams: $J_0 + J_8/J_{16}$, meter-long channels

Ref.: B. Miao et al., *Optical Guiding in Meter-Scale Plasma Waveguides*, Phys. Rev. Letts. 125, 074801 (2020).

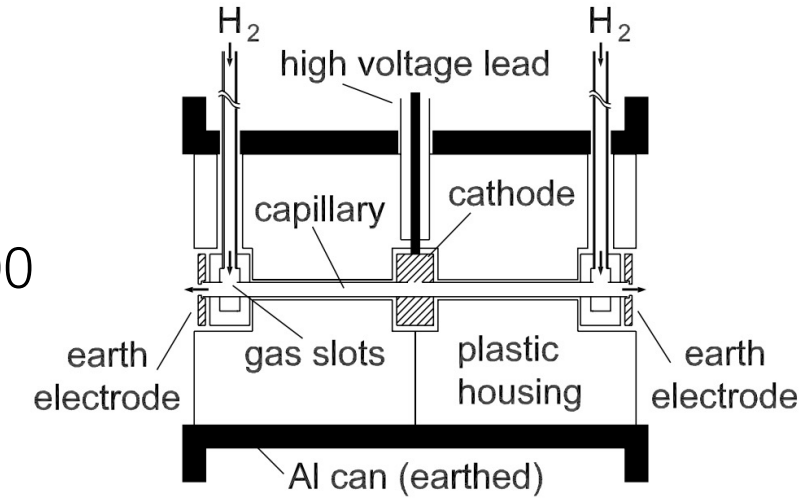

A. Butler et al., *Guiding of High-Intensity Laser Pulses with a Hydrogen-Filled Capillary Discharge Waveguide,* Phys. Rev. Letts. 89, 185003 (2002).

Long distance acceleration: Depletion

- **Pump-depletion:** properly select the pulse length to let the pump depletion length match the dephasing length

➢The front of the laser is not guided since the index of refraction requires a time to build up. (only for self-guiding)

➢Photon deceleration, absorption and other effects

- Etching velocity $v_{etch} \approx c\omega_p^2/\omega_0^2$
- Pump depletion length $L_{pd} \approx \frac{c}{v_{etch}} c\tau_{FWHM} \approx \frac{\omega_0^2}{\omega_p^2} c\tau_{FWHM} \geq L_d \approx \frac{2}{3}\frac{\omega_0^2}{\omega_p^2} R_b$

  where $R_b \approx 2\sqrt{a_0}c/\omega_p$
- Modified phase velocity of the wake

$$v_\phi \approx c\left(1 - \frac{1}{2}\frac{\omega_p^2}{\omega_0^2}\right) \Rightarrow v_\phi \approx c\left(1 - \frac{3}{2}\frac{\omega_p^2}{\omega_0^2}\right)$$

Long distance acceleration: experiment results

- 2006, LBNL, GeV energy barrier, external guiding: 38 fs, 25 micron, 40 TW; 4.3×10^{18} cm^{-3}, 3.3-cm-long
- 2009, the Rutherford Appleton Laboratory, ~GeV, self-guiding: 55 fs, 19 micron, >200 TW; 5.5×10^{18} cm^{-3}, 1-cm-long
- 2024, LBNL, **10 GeV**, external guiding: 40 fs, 53 micron, 500 TW; 10^{17} cm^{-3}, 30-cm-long

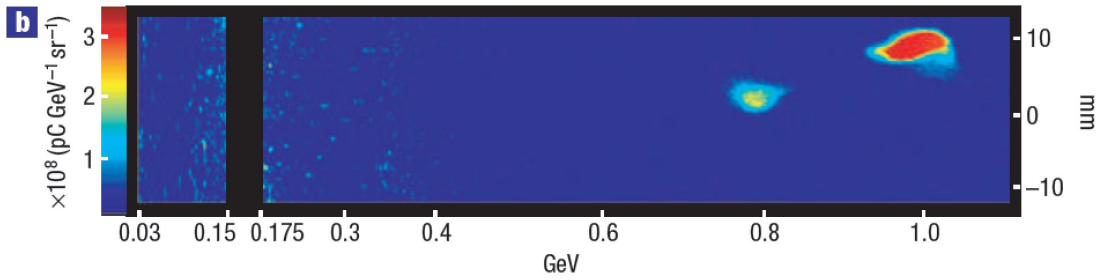

W. Leemans et al., *GeV electron beams from a centimetre-scale accelerator*, Nature Physics, 2, 696 (2006).

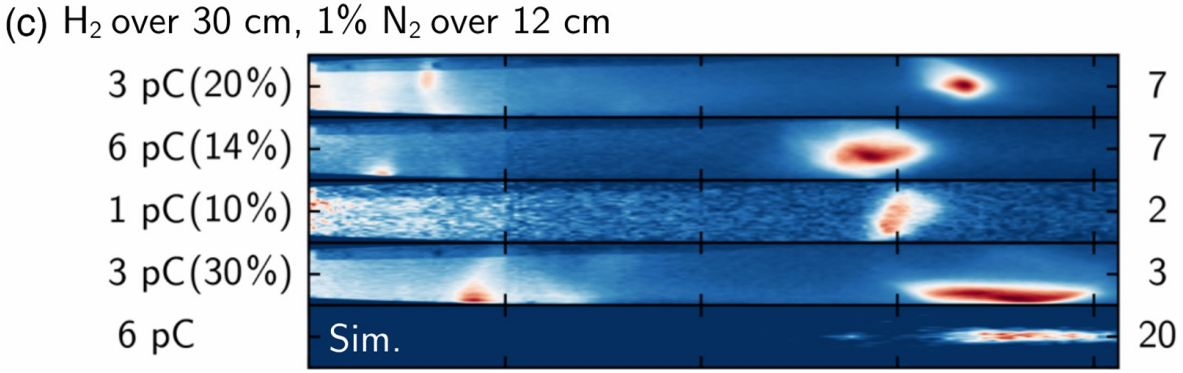

A. Picksley et al., *Matched Guiding and Controlled Injection in Dark-Current-Free, 10-GeV-Class, Channel-Guided Laser-Plasma Accelerators*, Phys. Rev. Lett. 133, 255001 (2024).

The Lawson-Woodward theorem

- The energy gain from a laser pulse in vacuum is **impossible** under the following conditions: **i)** the region of interaction is infinite; **ii)** the laser fields are in vacuum with no walls or boundaries present; **iii)** the electron is highly relativistic along the acceleration path; **iv)** no static electric or magnetic fields are present; and **v)** nonlinear effects (e.g., radiation reaction forces or ponderomotive force) are neglected.

Vacuum laser acceleration

Direct laser acceleration: from the laser electric field

Pondermotive acceleration

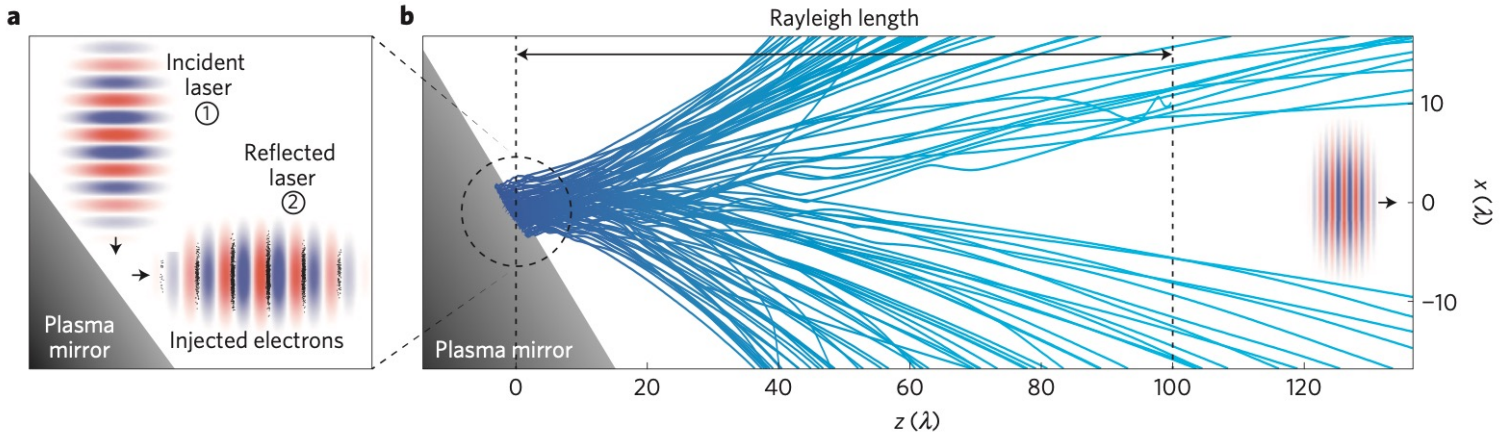

Refs: Chapter 3.4, P. Gibbon, Short Pulse Laser Interactions with Matter.

M. Thevenet *et al.*, *Vacuum laser acceleration of relativistic electrons using plasma mirror injectors*, Nature Physics 12, 355 (2015)

Outline

- Basics of Plasma-based acceleration
- **Injection: high-quality e^- beams**
- Applications of plasma-based acceleration

Injection Schemes

- Injection Condition: $\beta_z \geq \beta_{ph}$
- initial rest electrons, QSA: $\delta\psi \equiv \psi_f - \psi_i \approx -1$

Deviation can be found in the backup slides.

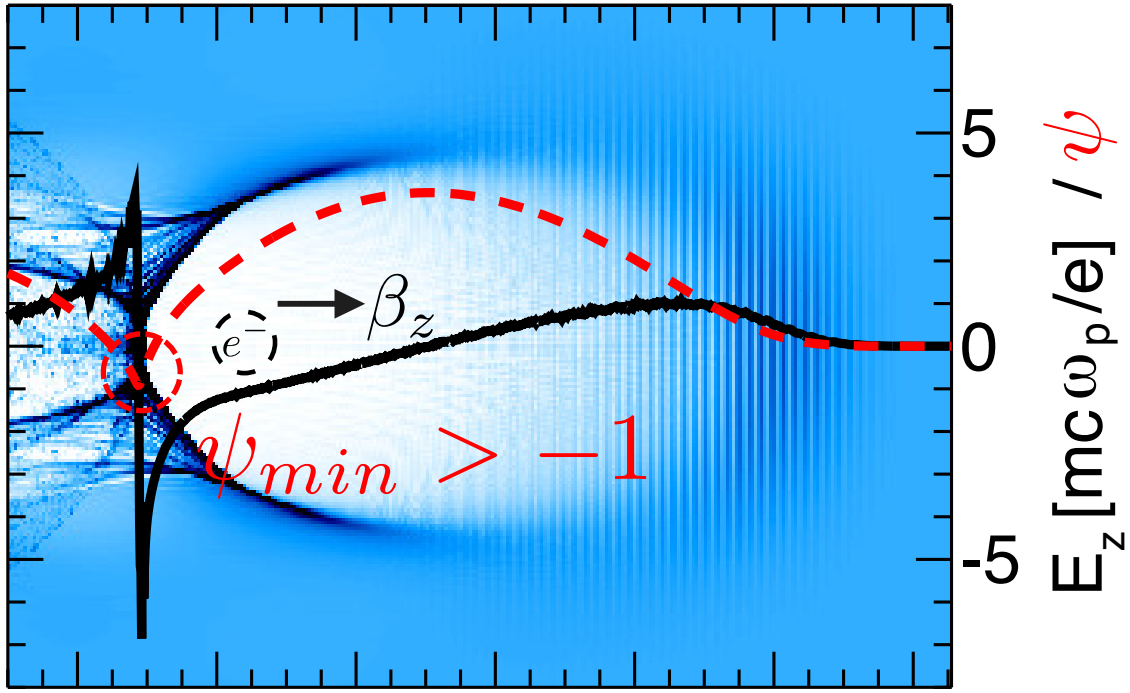

- External Injection
- Ionization Injection
- Density downramp injection
- Laser-Assisted Injection
- …

Ionization injection and its variation

- Key: a mixture of e^- with high and low ionization threshold
- Experiments: Oz et al. (beam-driven, Li + He), Pak et al. (laser-driven, He + N_2)
- The injection physics can be explained satisfactorily using $\delta\psi \approx -1$.

  - Driver: a_0=2, <500 mJ, 6 μm, ~45 fs (FWHM)
  - Plasma: 2mm, 90% He + 10% N_2, 7×10^{18} cm^{-3}
  - N_2: 14.5 eV, 29.6 eV, 47.4 eV, 77.5 eV, 97.9 eV, 552 eV, 667 eV.

A. Pak *et al., Injection and Trapping of Tunnel-Ionized Electrons into Laser-Produced Wakes*, Phys. Rev. Lett. 104, 025003 (2010).

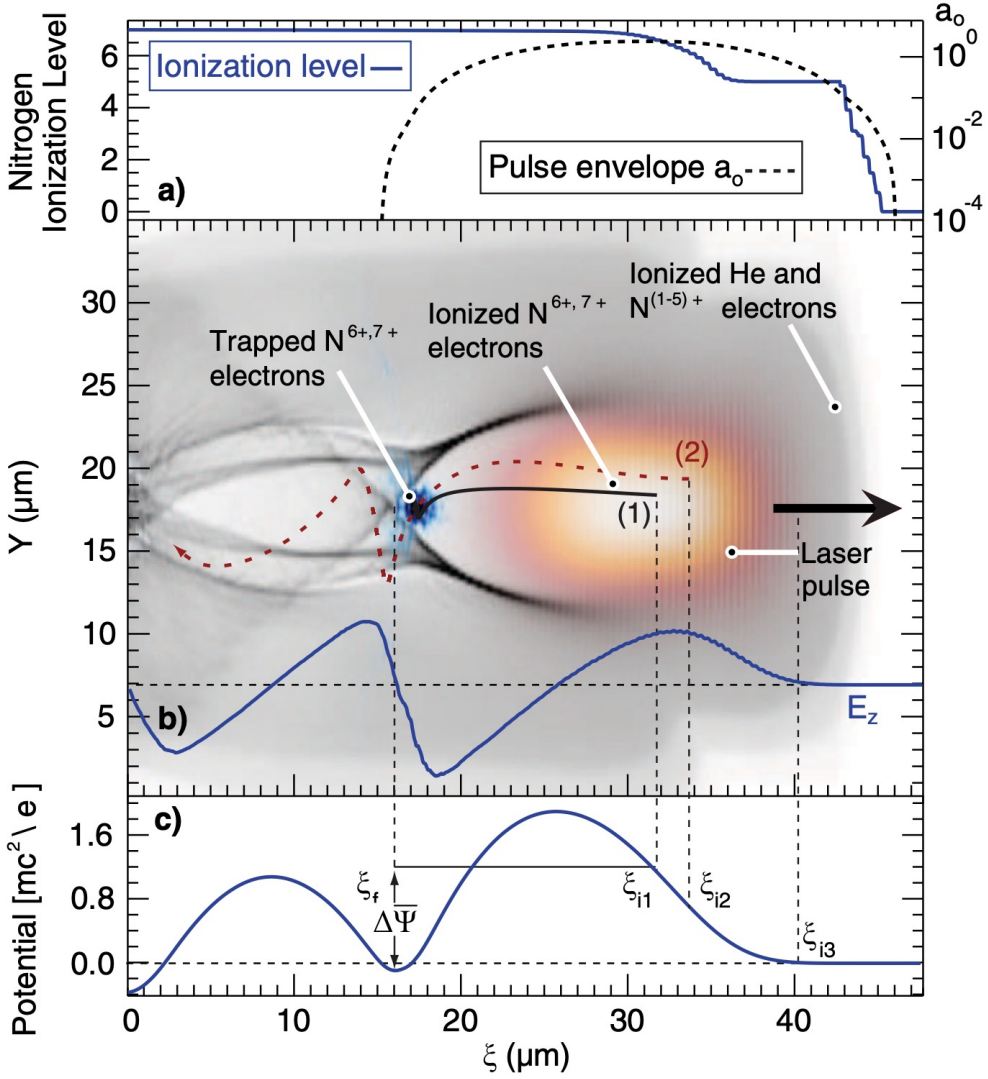

Ionization injection and its variation

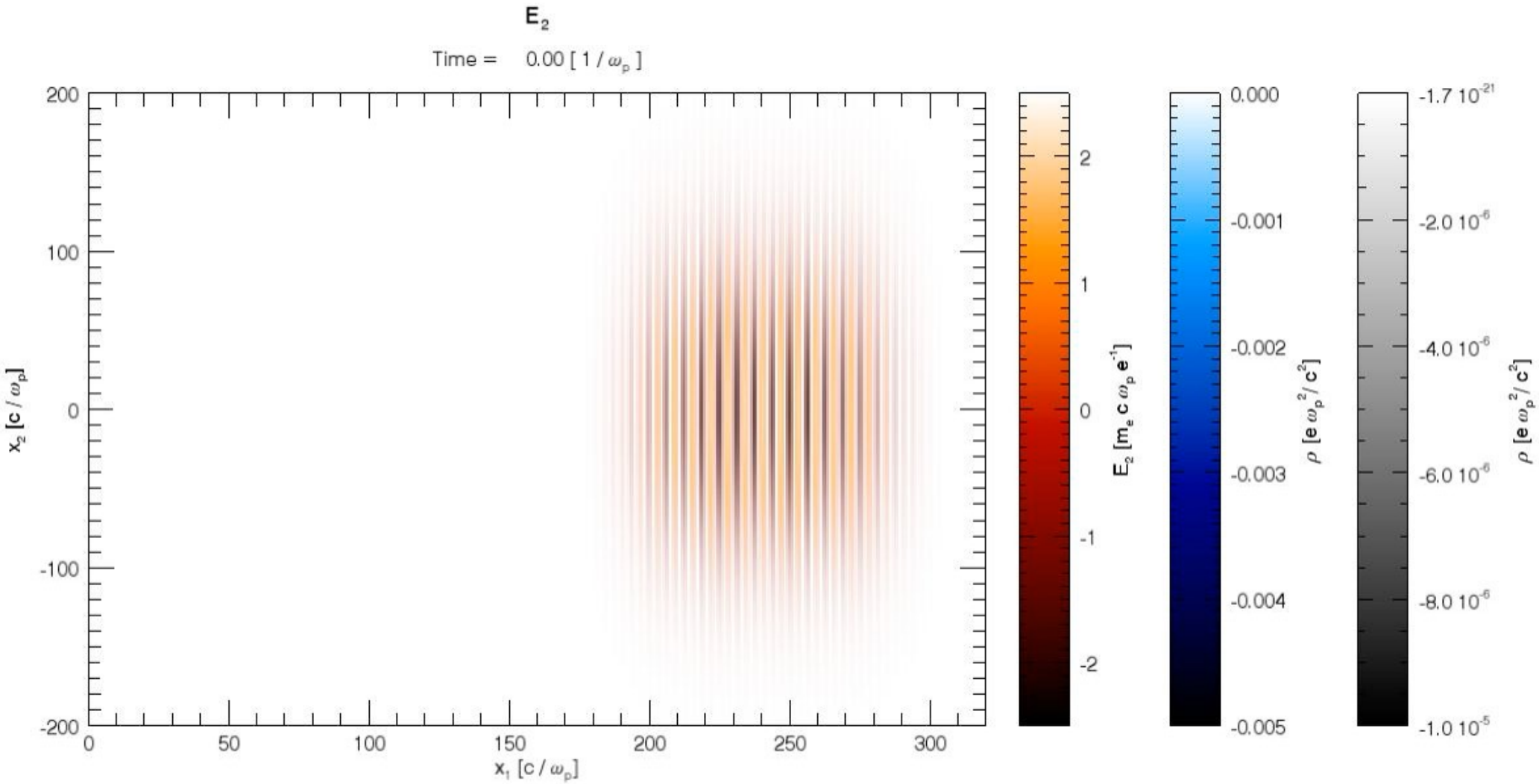

Ionization injection and its variation

- The requirements on the laser driver
  - ➢ Ionize the injected e^- (usually K-shell e^- of N)
  - ➢ Excite a wake with minimum $\delta\psi$<-1.

X. Xu *et al., Low emittance electron beam generation from a laser wakefield accelerator using two laser pulses with different wavelengths*, Phys. Rev. ST Accel. Beams 17, 061301 (2014).

Nitrogen and 800 nm lasers

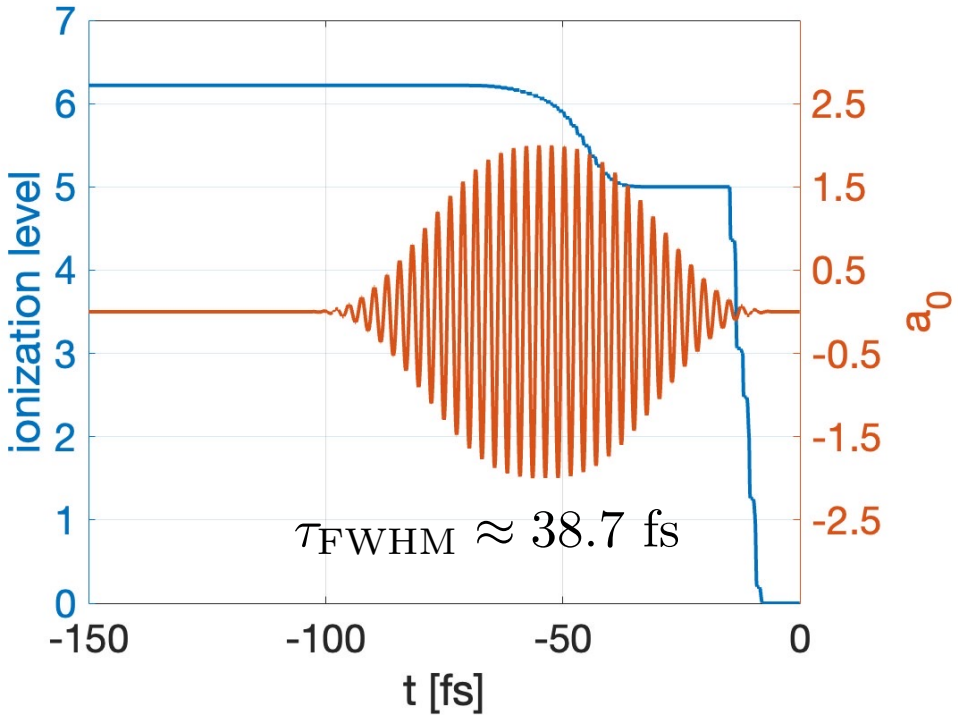

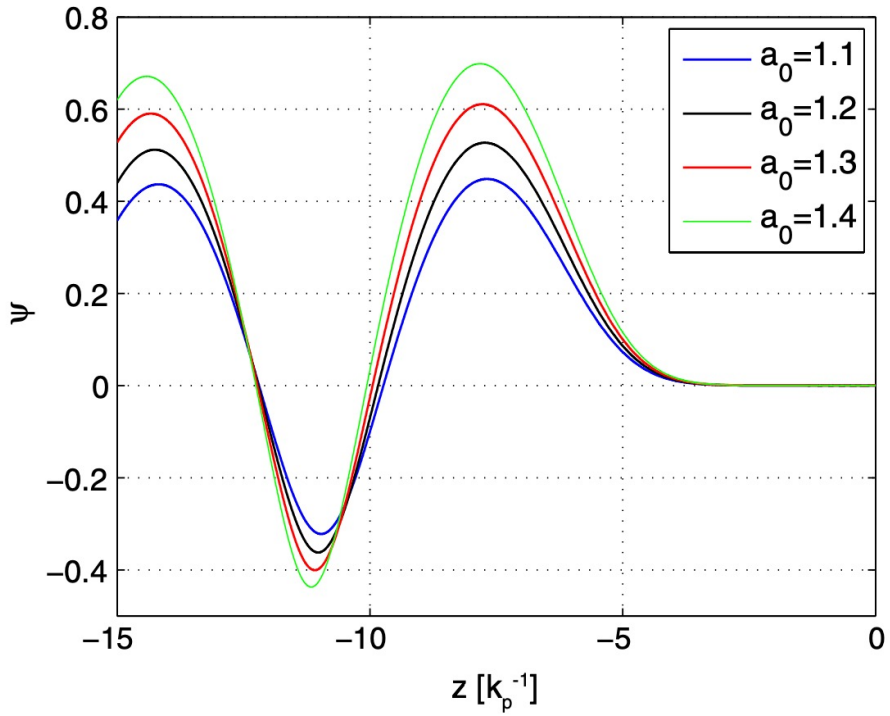

Ionization injection and its variation

- Use two or more pulses to separate the wake excitation and the injected e^- ionization.

  Injected e^-: μm transverse size

and 0.01mc $p_\perp$

- ➢ **Beam-driven laser-ionization**
- ➢ Two-color lasers

B. Hidding *et al., Ultracold Electron Bunch Generation via Plasma Photocathode Emission and Acceleration in a Beam-Driven Plasma Blowout,* Phys. Rev. Lett. 108, 035001 (2012).
Xinlu Xu, *et al., Phase-Space Dynamics of Ionization Injection in Plasma-Based Accelerators,* Phys. Rev. Lett. 112, 035003 (2014).

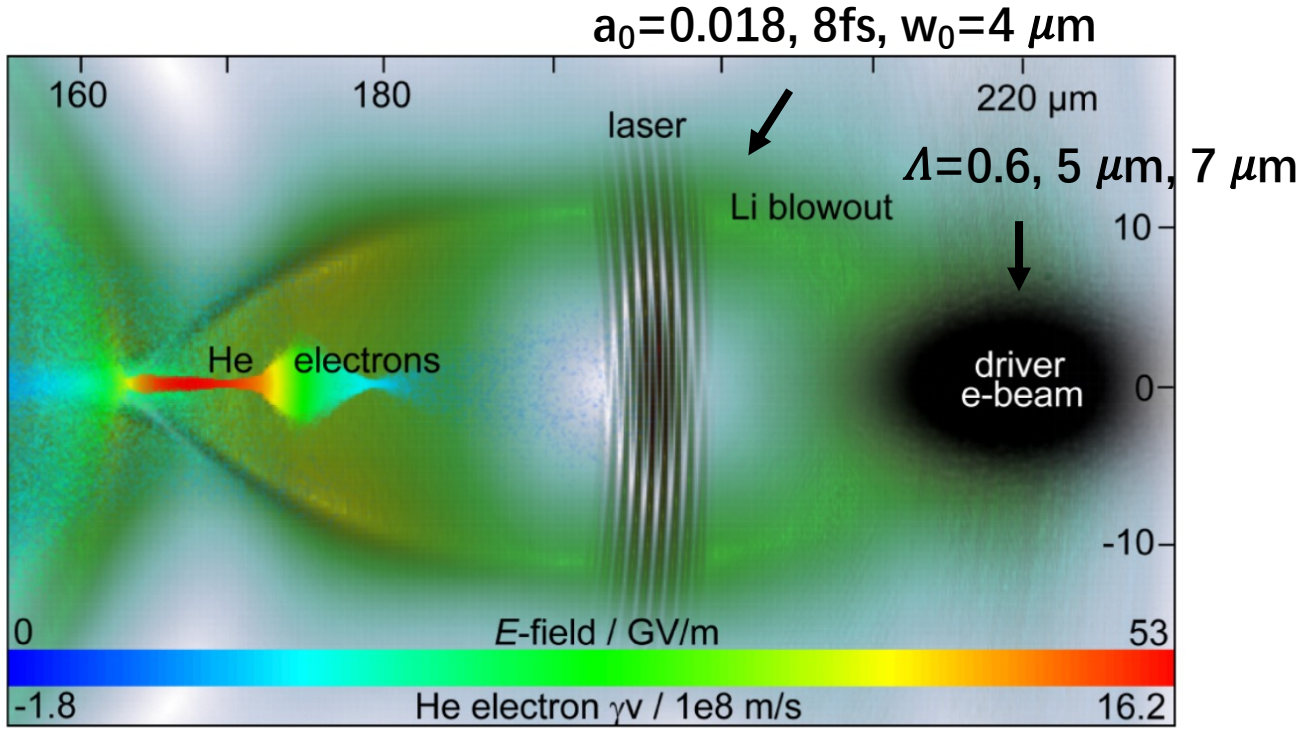

Plasma: $n_p=3.3\times10^{17}$ cm^{-3}
Injected e^- beam: **0.3 kA, ~30 nm, 2 pC, 7×10^{17} A/m²/rad²**

Ionization injection and its variation

- Use two or more pulses to separate the wake excitation and the injected e⁻ ionization.

➢ Beam-driven laser-ionization

➢ **Two-color lasers:** wake excitation depends on a while ionization depends on E

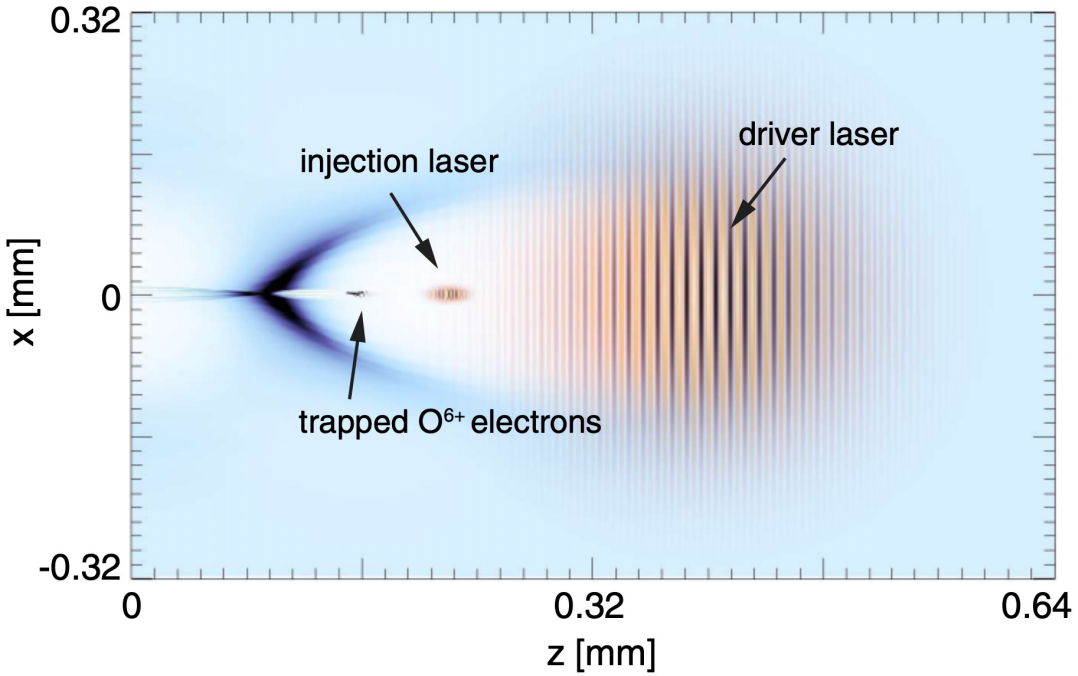

- ➢ Driver: 10 μm, a_0=1.4
- ➢ Injector: 400 nm, a_0=0.09;
- ➢ 10^{16} cm^{-3} Plasma + Oxygen

X. Xu, *et al., Low emittance electron beam generation from a laser wakefield accelerator using two laser pulses with different wavelengths*, Phys. Rev. ST Accel. Beams 17, 061301 (2014).

Ionization injection and its variation

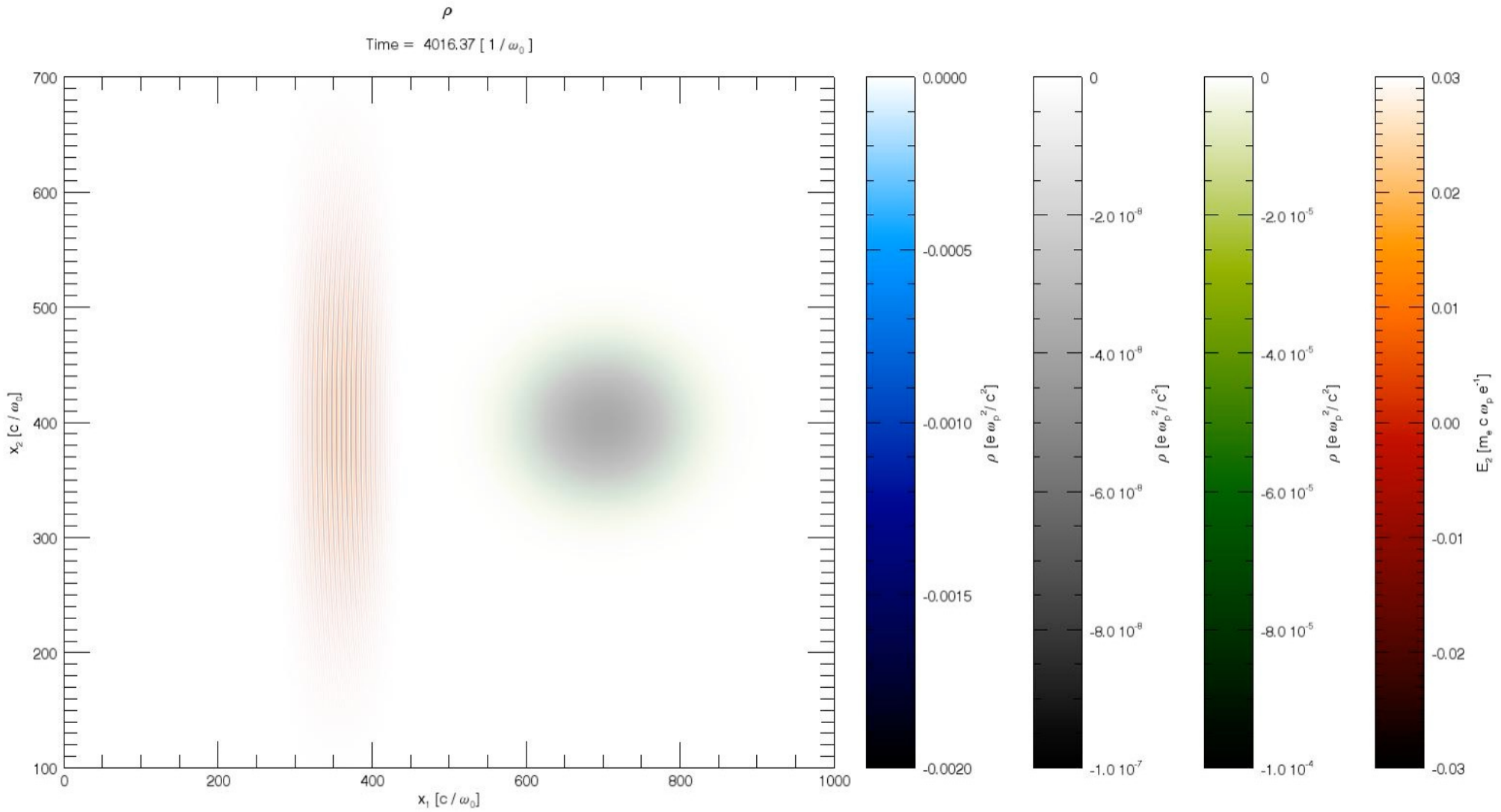

Bunched beam generation in ionization injection

- Based on the discrete tunneling ionization and the longitudinal mapping - Xinlu Xu, *et al., Nanoscale Electron Bunching in Laser-Triggered Ionization Injection in Plasma Accelerators,* Phys. Rev. Lett. 117, 034801 (2016).

$$\text{ionization rate} \propto \exp\left[-\frac{2(2I_p)^{3/2}}{3E_L}\right] \Rightarrow \text{discrete } \xi_i$$

$$\Downarrow \quad \xi_f \approx \sqrt{4+\xi_i^2}$$

discrete ξ_f

- High-dimensional effects limit the wave number of the modulation between $2k_0$ and $5k_0$.

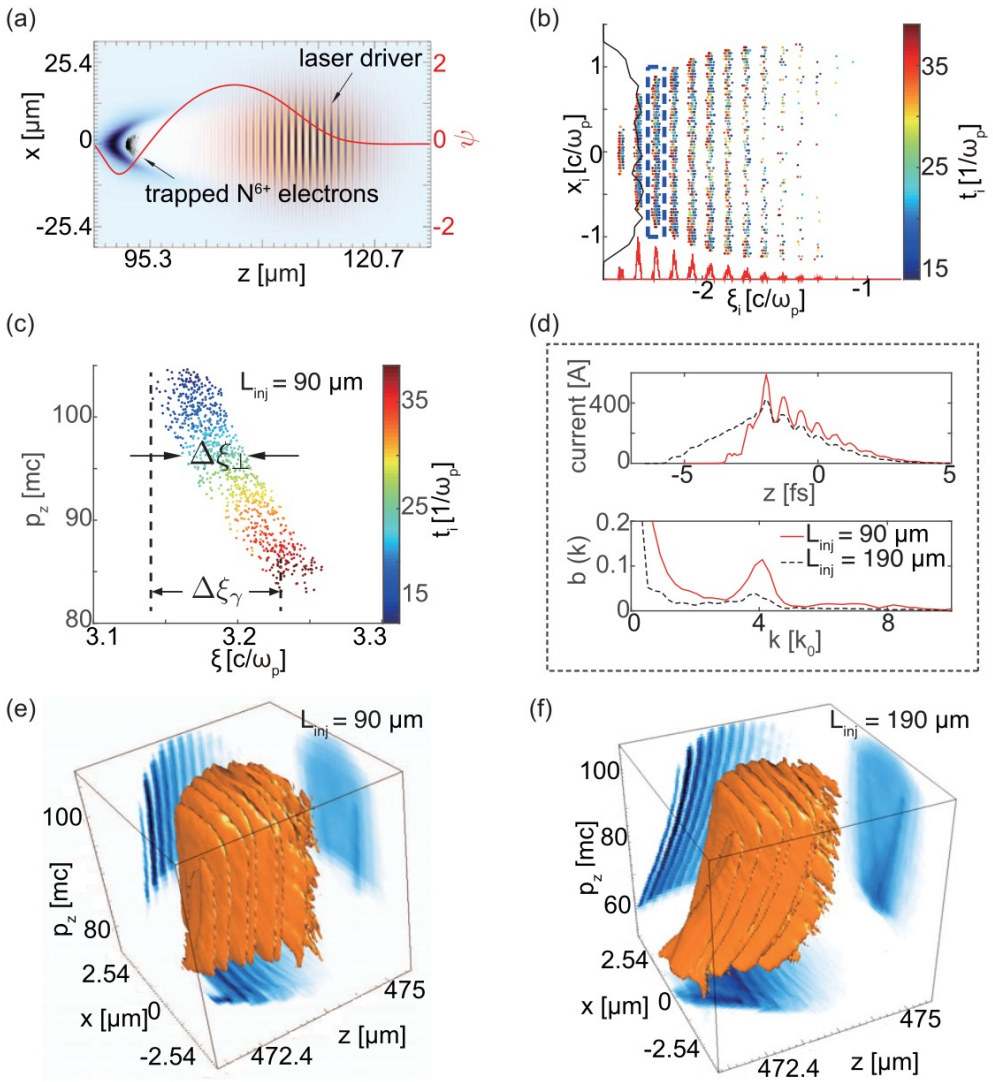

Density Downramp injection (DDI)

- Use a plasma density downramp to reduce the wake phase velocity.

$$\phi(z,t) = \omega_p(z)(z/v_d - t)$$

$$v_{ph}(z,t) = \frac{v_d}{1 - (\mathrm{d}\omega_p/\mathrm{d}z)\omega_p^{-1}(v_d t - z)}$$

- The original idea of DDI was proposed in S. Bulanov, *et al.,* Phys. Rev. E 58, R5257 (1998) (slow ramp) and H. Suk, *et al.,* Phys. Rev. Lett. 86, 1011 (2001) (sharp ramp).

$$l \equiv \left| \frac{n_p}{\mathrm{d}n_p/\mathrm{d}z} \right| \gg \text{ or } \ll \lambda_{wake}$$

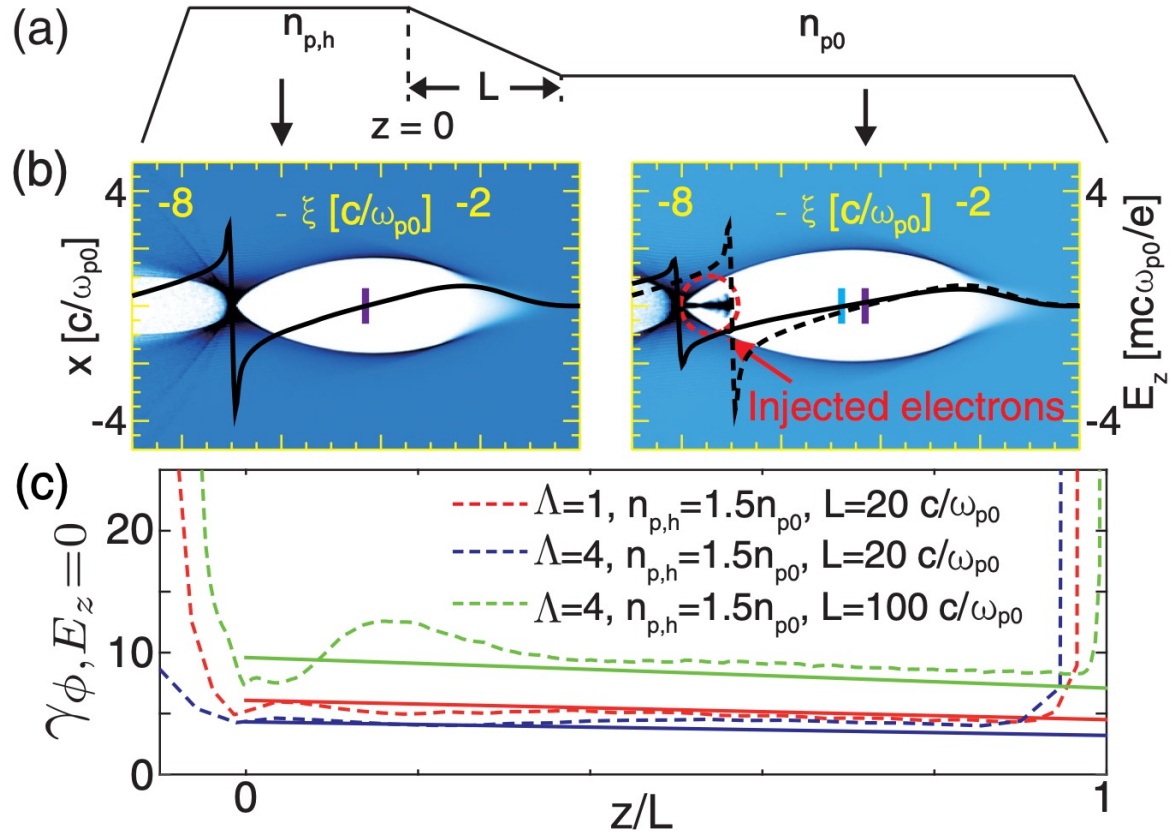

Xinlu Xu, *et al.,* Phys. Rev. Accel. Beams 20, 111303 (2017).

Density Downramp injection (DDI)

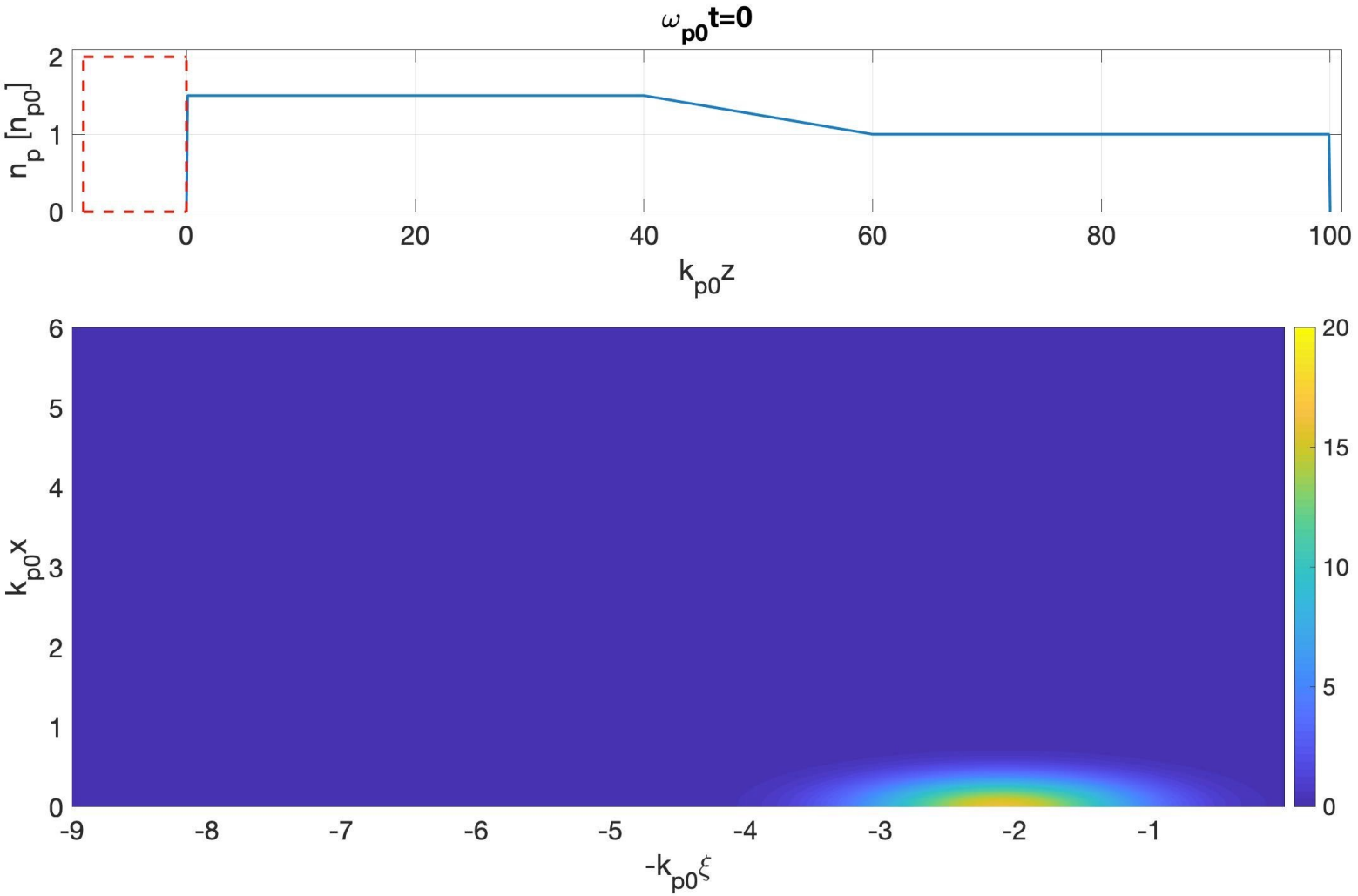

Phase space dynamics in DDI

- Two important dynamics of the injected e^- : Transverse deceleration and longitudinal mapping

➢Transverse deceleration

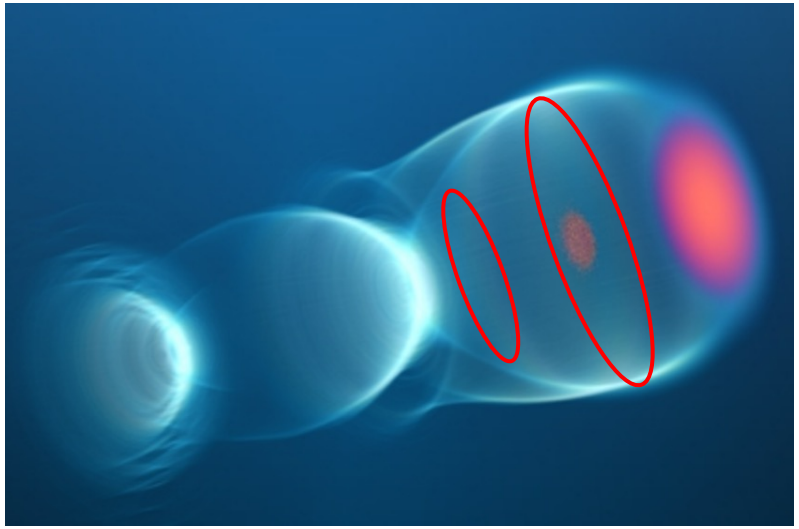

ring-shaped distribution before injection

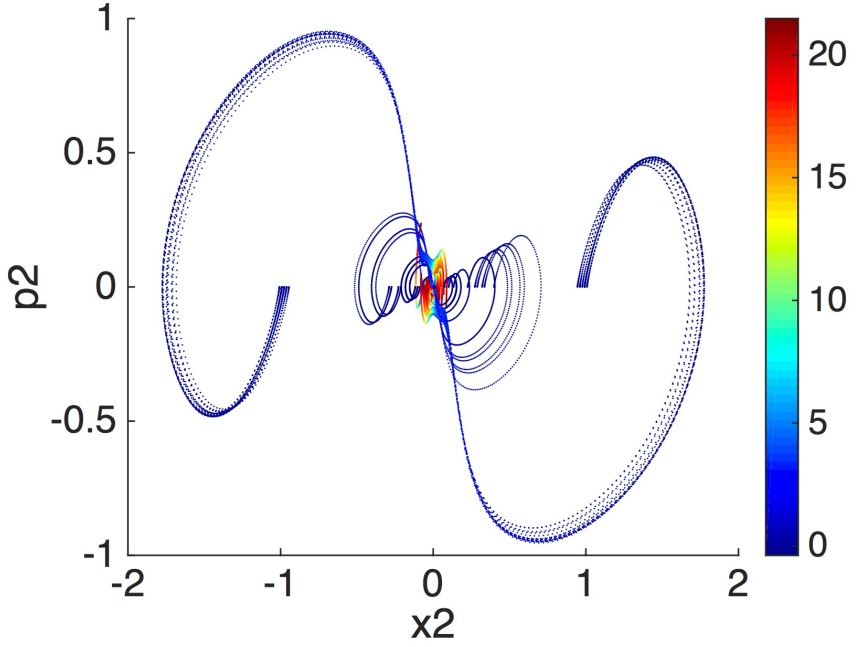

Trajectories of the injected e^-

➢ Low emittance beam

$\epsilon_N \sim 0.01c/\omega_p$

~20 nm@10^{19} cm^{-3}

Xinlu Xu, *et al., High quality electron bunch generation using a longitudinal density-tailored plasma-based accelerator in the three-dimensional blowout regime,* Phys. Rev. Accel. Beams 20, 111303 (2017).

Phase space dynamics in DDI

- Longitudinal Mapping

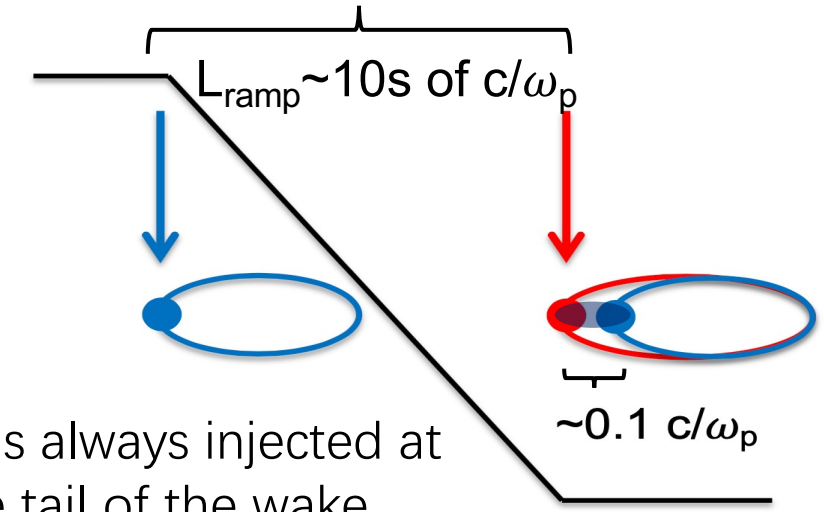

e^- is always injected at the tail of the wake.

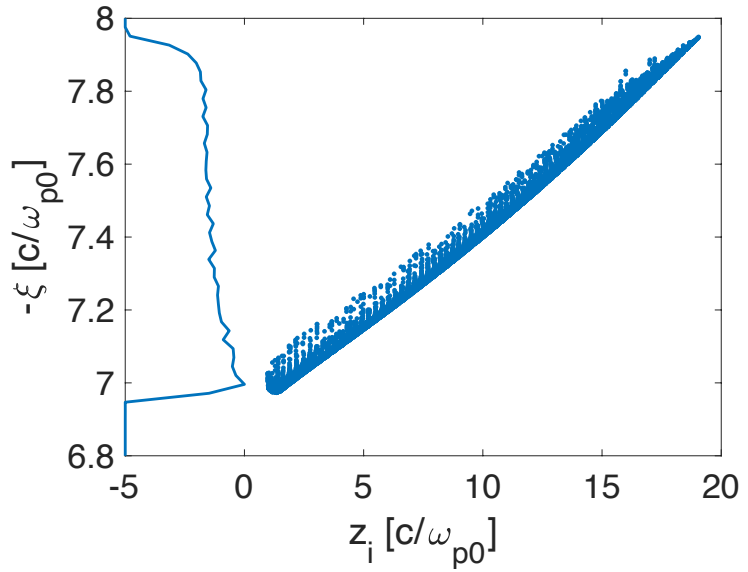

Longitudinal phase mixing is broken!

- Slice energy spread: $O(0.1)$ MeV!
- Energy chirp: high energy head and low energy tail.
- High current due to the compression: $I \approx I_d/2$ or $(a_0/4)I_A$

Phase space dynamics in DDI: pre-bunched

Turn the injection on and off periodically to form a pre-bunched beam

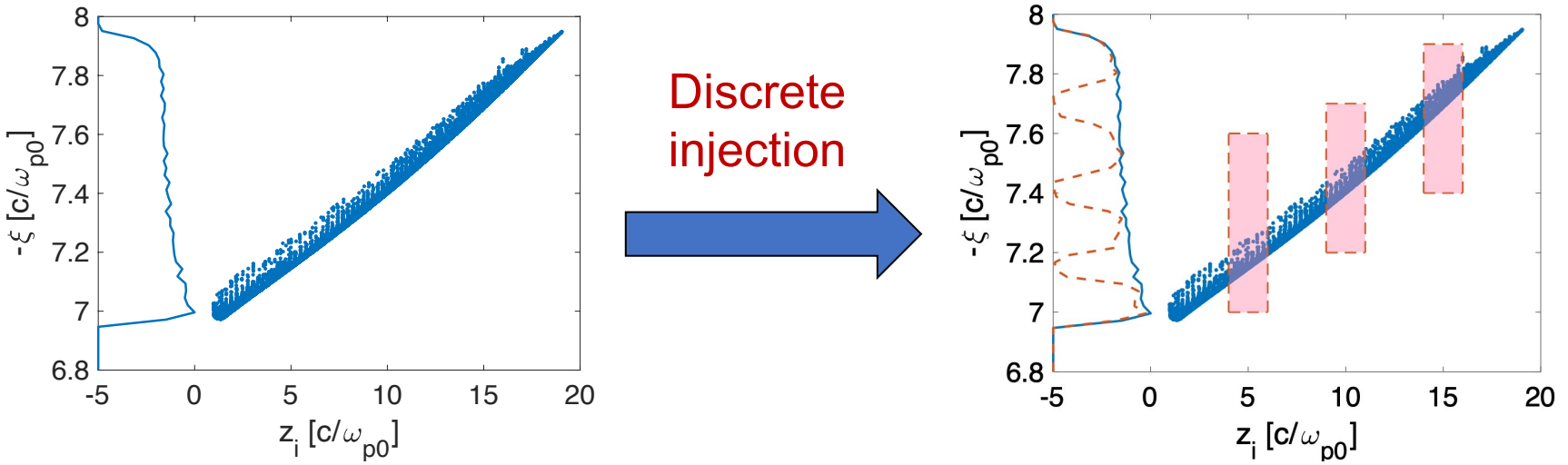

The period is significantly compressed with a compression factor of $O(100)$.

Xinlu Xu, *et al., Generation of ultrahigh-brightness pre-bunched beams from a plasma cathode for X-ray free-electron lasers,* Nature Communications 13, 3364(2022).

Phase space dynamics in DDI: pre-bunched

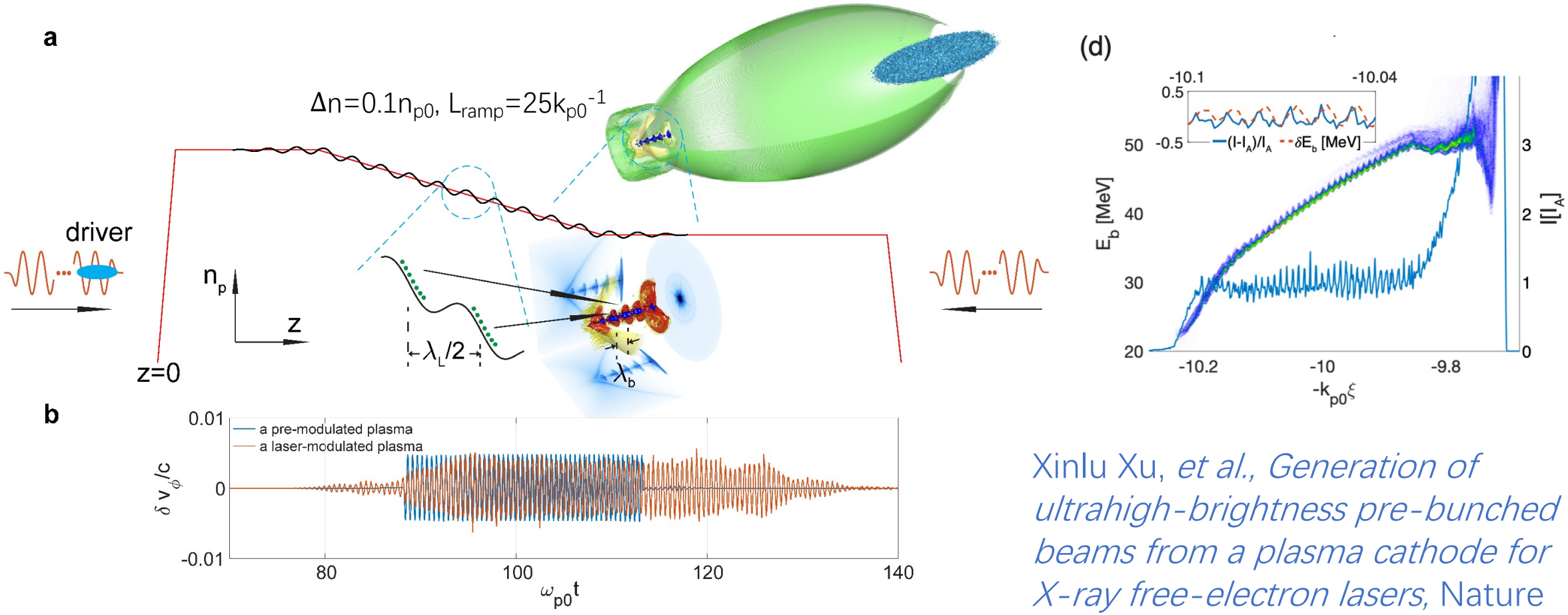

Xinlu Xu, *et al., Generation of ultrahigh-brightness pre-bunched beams from a plasma cathode for X-ray free-electron lasers,* Nature Communications 13, 3364(2022).

Variants of DDI

- The key is to increase the wake size slowly.

A evolving electron beam driver in a uniform plasma: focused using external optics[1], self-focused[1], flying-focused[2]

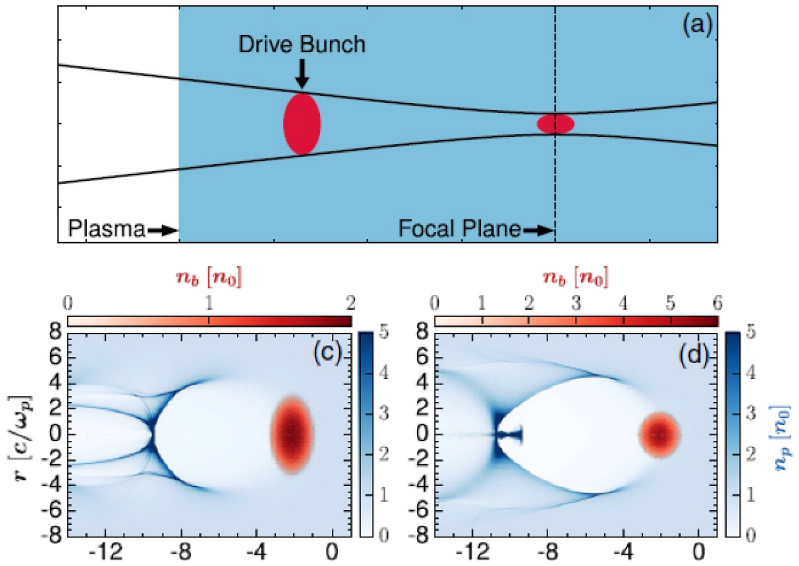

A evolving laser driver in a uniform plasma[3]

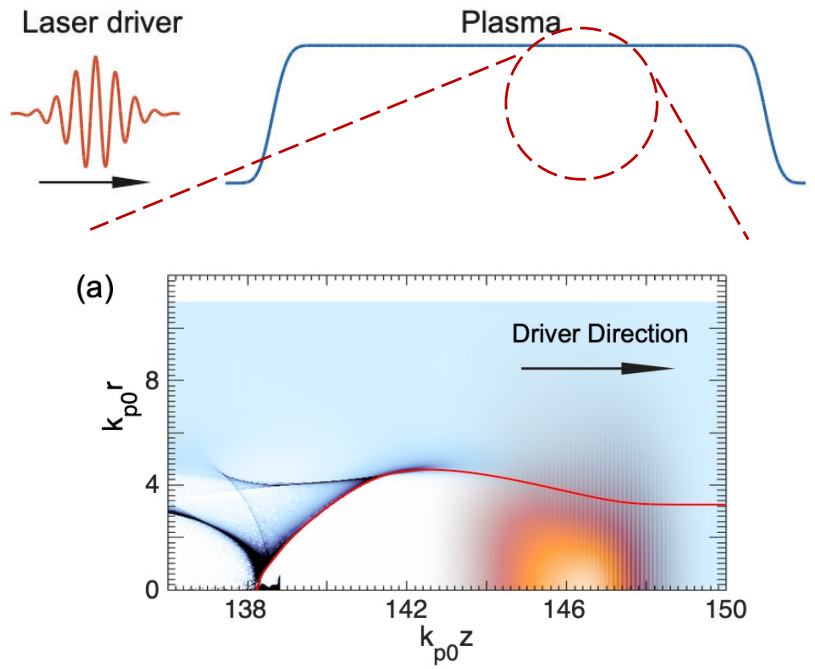

[1]T. N. Dalichaouch *et al.,* Phys. Rev. Accel. Beams 23, 021304 (2020);
[2]F. Li *et al.,* Phys. Rev. Lett. 128, 174803 (2022).

[3]X. Xu *et al.,* Phys. Rev. Accel. Beams 26, 111302 (2023).

Experimental results of DDI

- Stable beams with low energy spread.

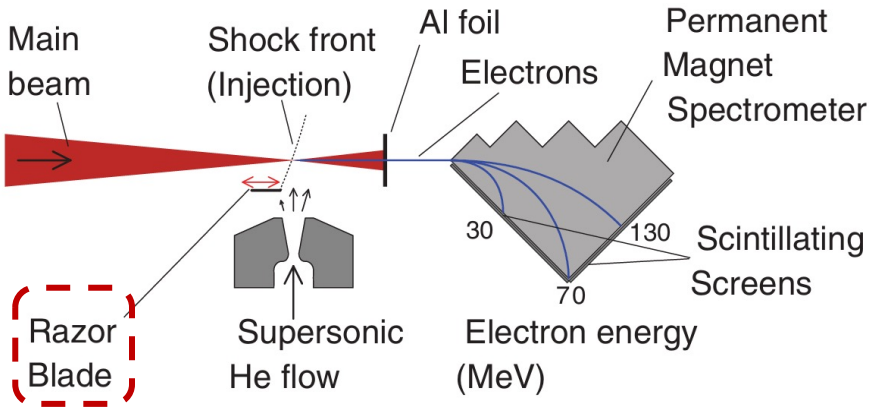

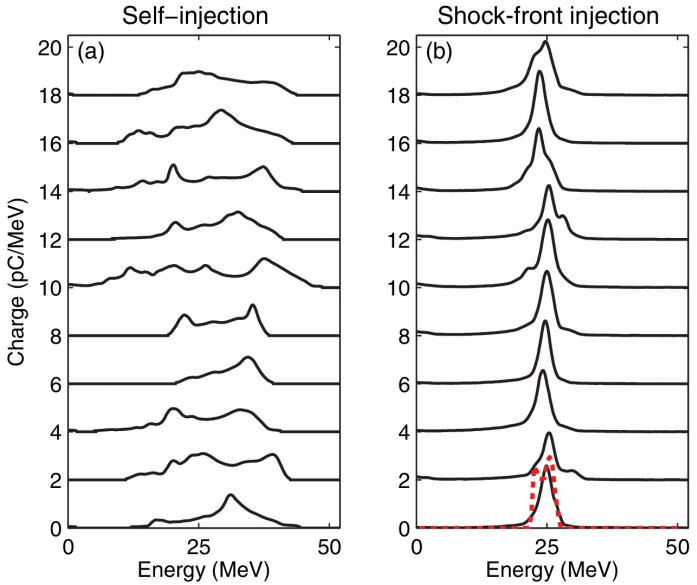

➢ 770 mJ, 28 fs, a FWHM spot size of 13.5 μm, an intensity of 4×10^{18} W/cm^2 (a_0=2).

1.2×10^{19} cm^{-3} 0.6×10^{19} cm^{-3}

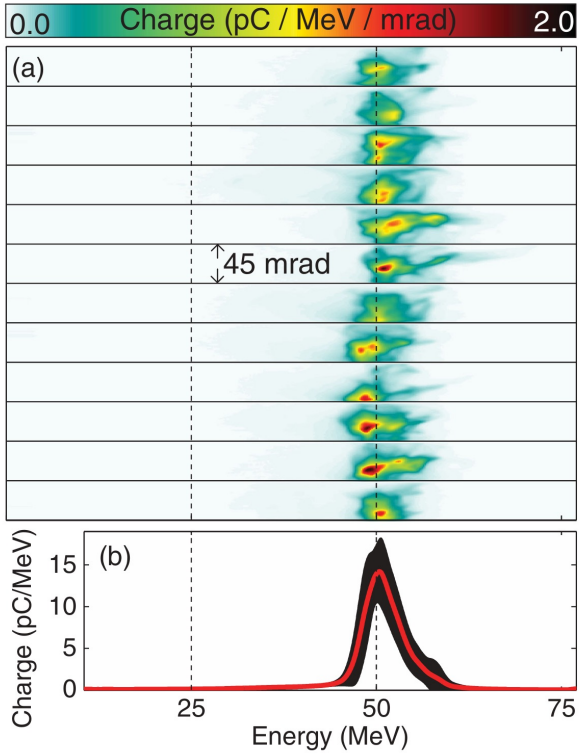

➢ A laser upgrade: 1200 mJ, (a_0=2.5)

K. Schmid *et al., Density-transition based electron injector for laser driven wakefield accelerators,* Phys. Rev. Accel. Beams 13, 091301 (2010); A. Buck *et al., Shock-Front Injector for High-Quality Laser-Plasma Acceleration*, Phys. Rev. Lett. 110, 185006 (2013).

Experimental results of DDI

- Stable beams with low energy spread and **low emittance**.

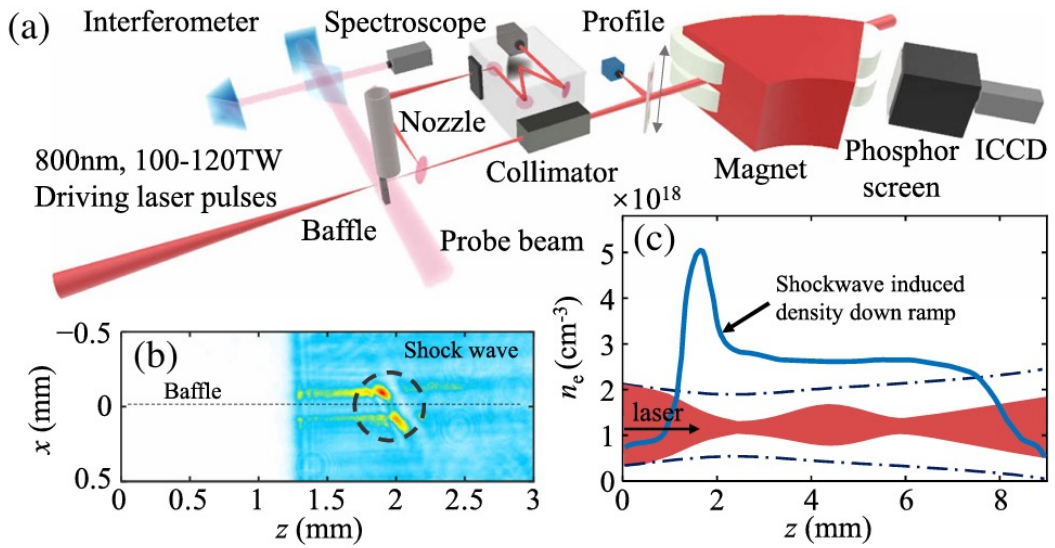

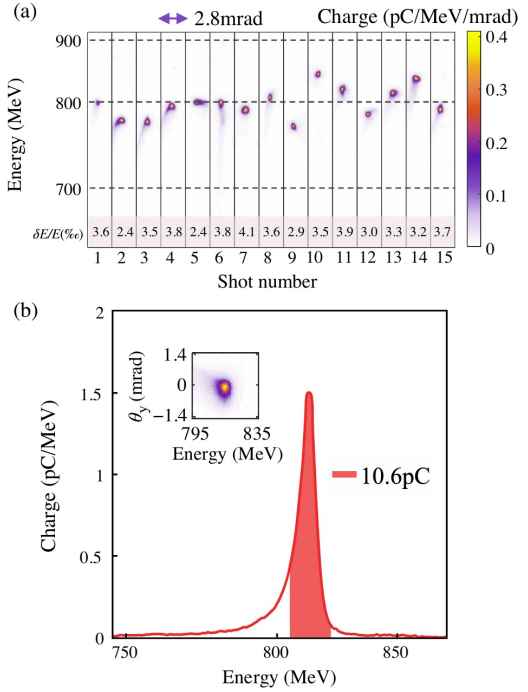

- 780–840 MeV,
- rms energy spreads of 2.4‰–4.1‰,
- charges of 8.5–23.6 pC,
- rms divergences of 0.1–0.4 mrad

- 100~120 TW, 25-fs, a FWHM spot size of 40/38 μm, an intensity of ~3×10^{18} W/cm^2 (a_0=1.2 or 1.3).

W. Wang *et al., High-Brightness High-Energy Electron Beams from a Laser Wakefield Accelerator via Energy Chirp Control,* Phys. Rev. Lett. 117, 124801 (2016); L. Ke *et al., Near-GeV Electron Beams at a Few Per-Mille Level from a Laser Wakefield Accelerator via Density-Tailored Plasma,* Phys. Rev. Lett. 126, 214801 (2021); W. Wang *et al., Free-electron lasing at 27 nanometres based on a laser wakefield accelerator,* Nature 595, 516 (2021).

Outline

- Basics of Plasma-based acceleration
- Injection: high-quality e^- beams
- **Applications of laser plasma acceleration**

X/γ-ray sources: betatron motion

- Ultrafast duration: ~fs, suitable for ultrafast science
- Small source size: ~μm, suitable for phase contrast imaging
- Spectrum: 10s of keV, ~10^9

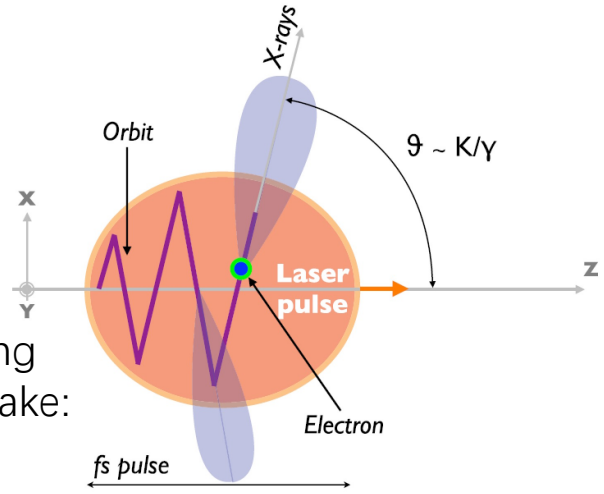

Strong focusing force in the wake: >MT/m

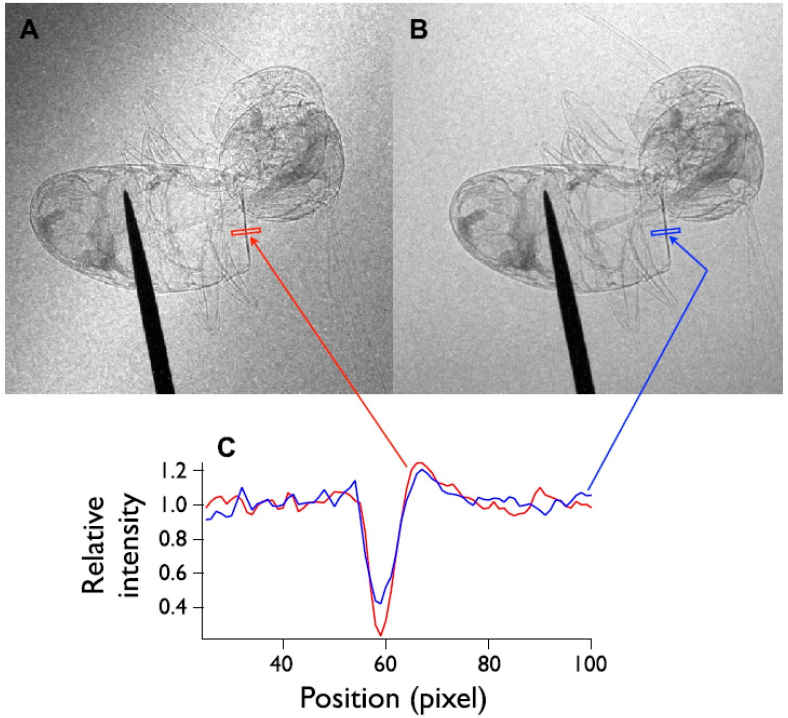

S. Corde et al., *Femtosecond x rays from laser-plasma accelerators,* Review of Modern Physics 85, 1 (2012).

Compact free-electron lasers

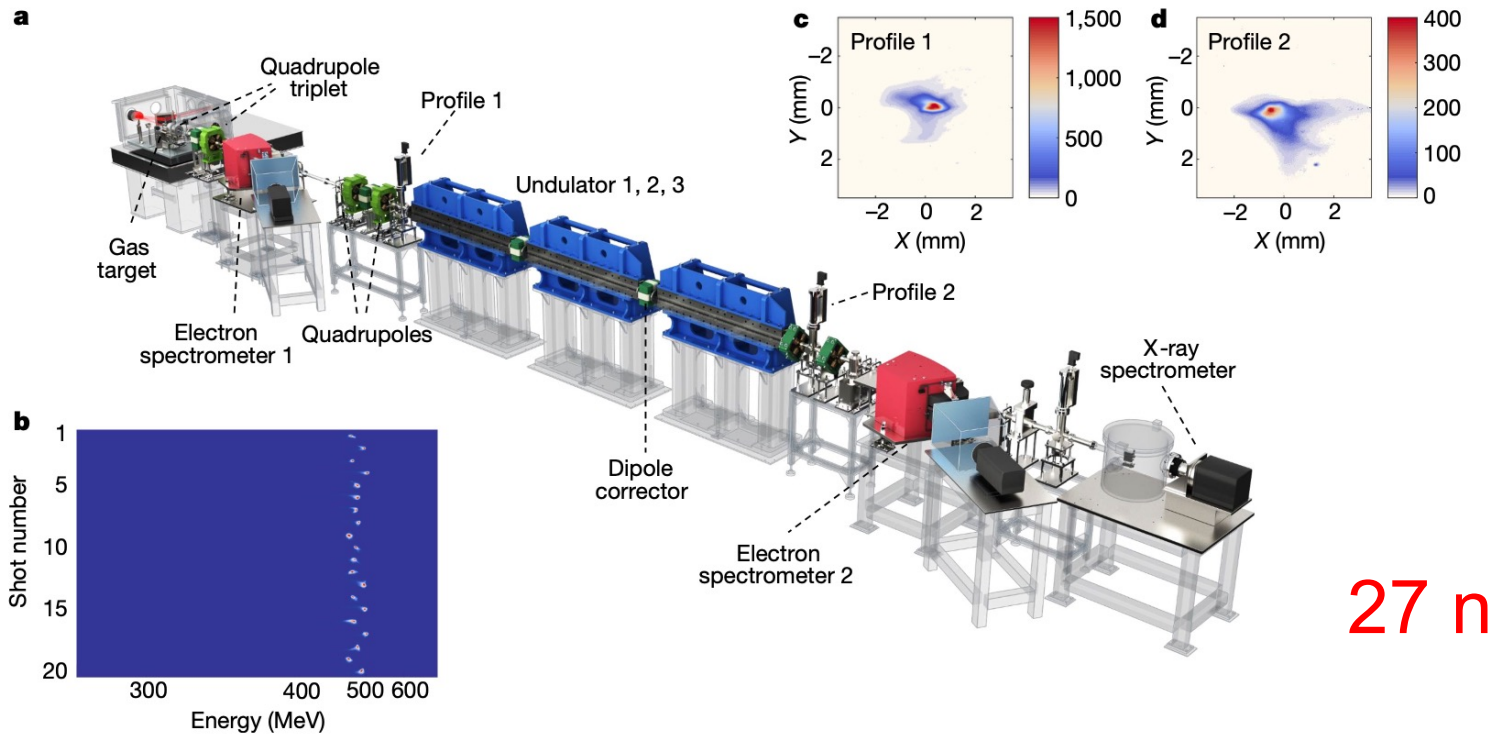

27 nm !

Wentao Wang, et al., *Free-electron lasing at 27 nanometres based on a laser wakefield accelerator,* Nature 595, 516 (2021).

Quantum electrodynamics (QED) study

- The critical field of QED $E_{cr}=1.3\times10^{18}$ V/m.
- Collision between high-energy electrons (>~GeV) and high-intensity laser (a_0>~10)can access QED regime.

➢In the beam rest field, the laser field is enhanced by a factor of γ.

➢1996, SLAC: 46.6 GeV electron beam and TW laser (a_0~0.5)

➢2018, Rutherford Appleton Laboratory: ~GeV electron beam + laser with a_0=21

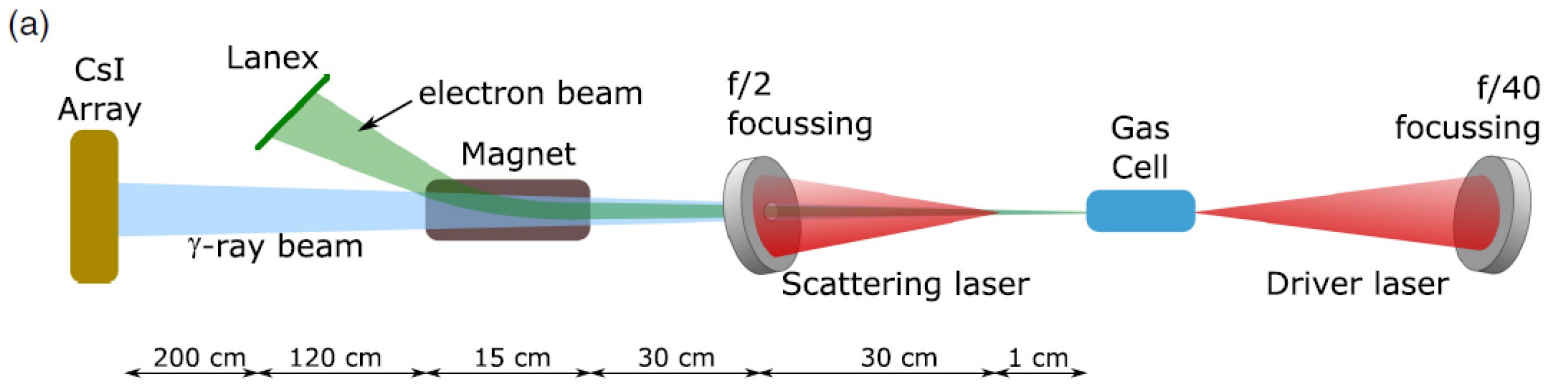

J. Cole et al., PRX 8, 011020 (2018; K. Poder, PRX 8, 031004 (2018).

12TH INTERNATIONAL ORGANIZATION OF CHINESE PHYSICISTS AND ASTRONOMERS ACCELERATOR SCHOOL

OCPA-2025

KHAOYAI, NAKHON RATCHASIMA, THAILAND
29 JULY - 7 AUGUST 2025

Thanks!

Xinlu Xu
xuxinlu@pku.edu.cn

Normalization

- We usually use the plasma density n_0 and the related quantities as the normalized units.

➢ Density: n_0;

➢ Speed: c ; Length: c/ω_p; Time: $1/\omega_p$;

➢ Electric field: $mc\omega_p/e$; Magnetic field: $m\omega_p/e$;

➢ Scalar Potential: $m_e c^2/e$; Vector Potential: $m_e c/e$;

➢ Charge: e; Momentum: $m_e c$;

Normalization

Large n_0

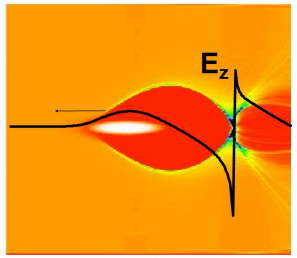

Small n_0

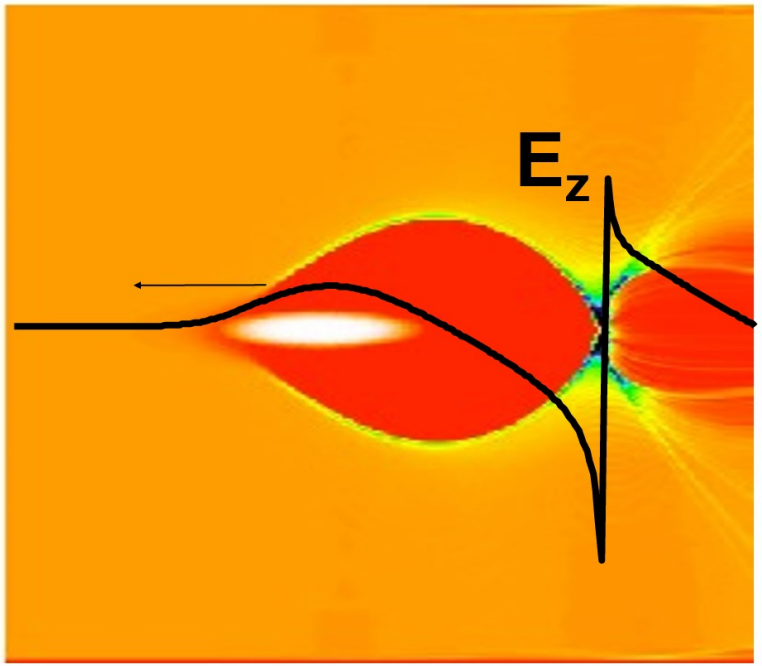

- **Beam driver:** if $k_p\sigma_r$, $k_p\sigma_z$ and I ($\Lambda=2I/I_A$) of the driver are the same, the excited wakefield in normalized units [e.g., k_pR_b, $E_z/(mc\omega_p/e)$] is the same.
- **Laser driver:** if $k_p\sigma_r$, $k_p\sigma_z$, $k_p\lambda_L$ and $E_L/(mc\omega_p/e)$ of the driver are the same, the excited wakefield in normalized units [e.g., k_pR_b, $E_z/(mc\omega_p/e)$] is the same. However, since the ponderomotive force plays the role for wake excitation, we actually need $k_p\sigma_r$, $k_p\sigma_z$ and $a_0=E_L/(mc\omega_L/e)$ the same.
- Note Λ and a_0 are the same when using different plasma density as the normalized unit.

On the injection condition $\delta\psi \approx -1$

- A conservation quantity under the QSA: $\gamma m_e c^2 - p_z c - e\psi = \text{constant}$

➢For an initially rest electron: $\gamma - \beta_\phi p_z - \psi = 1 - \psi_0$

$$\gamma^2 = 1 + p_z^2 + p_\perp^2$$
$$\beta_z = \beta_\phi$$

$$1 + \delta\psi = \frac{\sqrt{1 + p_\perp^2}}{\gamma_\phi}$$

➢For large γ_ϕ and small $p_\perp$, we get the injection condition $\delta\psi \approx -1$.

➢It is easier to get injection at higher plasma density since the γ_ϕ is lower.

External injection: Beam-driven

- e^- sources: conventional RF accelerators or plasma-based accelerators
- Challenges: compress the beam to 10s of micron in each dimension

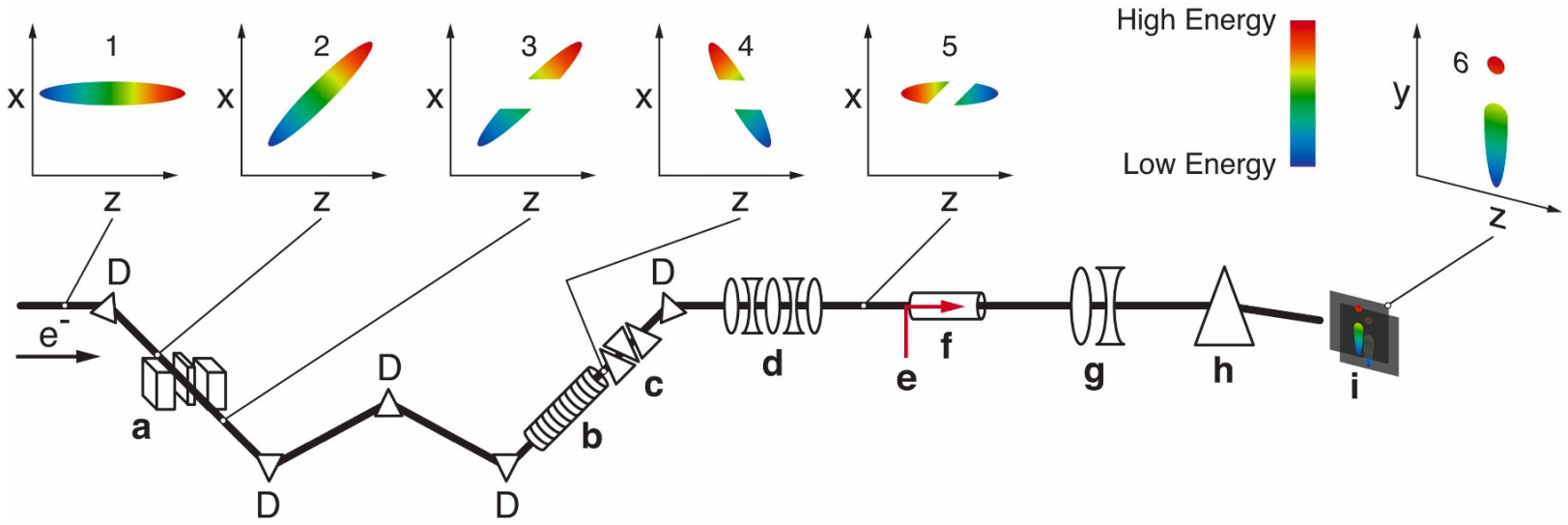

Extended Data Figure 1 | FACET experimental area schematic. Electron beam line features: **a**, beam notching device, **b**, transverse deflecting structure, **c**, initial spectrometer, **d**, final-focus quadrupole magnets, **e**, lithium plasma ionization laser, **f**, lithium vapour column, **g**, spectrometer imaging quadrupole magnets, **h**, spectrometer dipole magnet, and **i**, Cherenkov and phosphor screens. Bend dipole magnets in the 'W'-shaped chicane are each labelled 'D'. The arrow beneath the e^- symbol indicates the electron beam's direction of motion (left to right).

- Driver: 25 μm, 4.5 kA
- Witness: 47 μm, 2 kA
- 5×10^{16} cm^{-3}, 36-cm-long

M. Litos *et al., High-efficiency acceleration of an electron beam in a plasma wakefield accelerator*, Nature, 515, 92, 2014

External injection: Laser-driven

- e^- sources: conventional RF accelerators or plasma-based accelerators
- Challenges: compress the beam to 10s of micron in each dimension

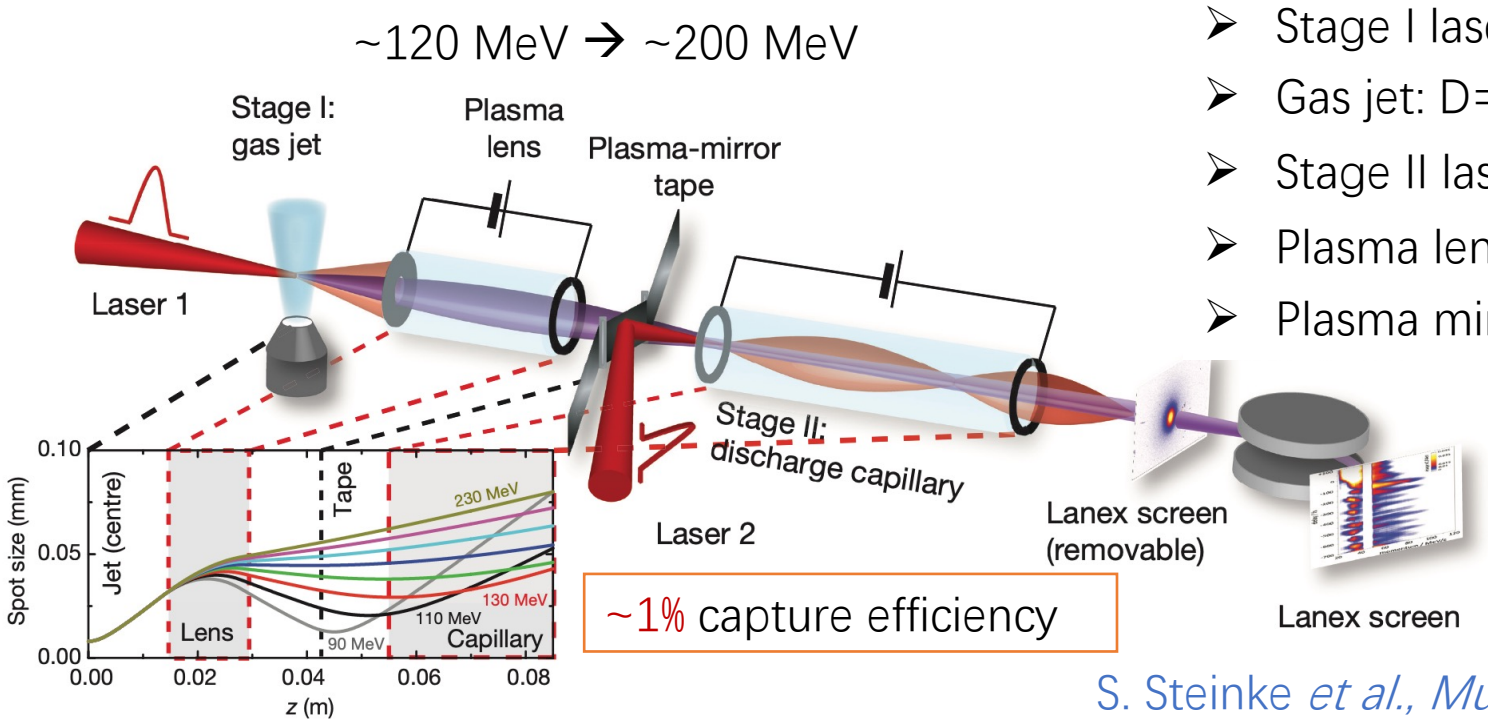

~1% capture efficiency

- Stage I laser: 45 fs, 1.3 J, 18 μm, 4×10^{18} W/cm^2
- Gas jet: D=700 μm, 5×10^{18} cm^{-3}, He+N
- Stage II laser: 45 fs, 0.45 J, 18 μm, 1.4×10^{18} W/cm^2
- Plasma lens: 15-mm-long, D=500 μm
- Plasma mirror: 80% laser energy throughput

S. Steinke *et al., Multistage coupling of independent laser-plasma accelerators*, Nature, 530, 190, 2016

Colliding pulse injection

- One intense laser pulse excites a wake and one or more weak laser pulses alters the electrons' trajectories and some of them can be trapped.

➢ 1996, D. Umstadter, et al., one pump laser + one perpendicularly propagating injection laser

➢ 1997, E. Esarey, et al., one pump laser + two counterpropagating injection pulses

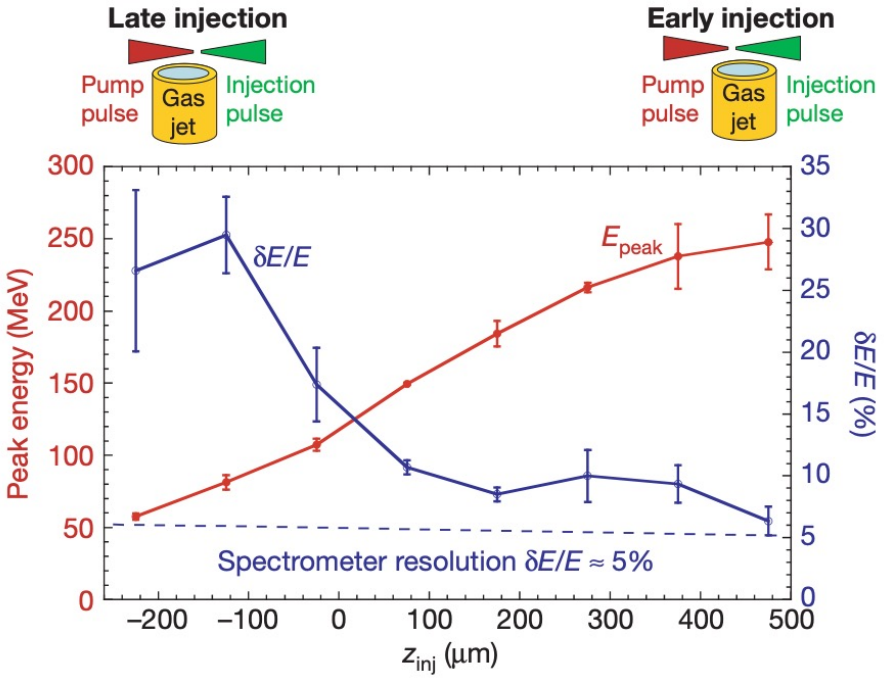

- ❑ Two lasers: a_0=1.3, a_1=0.4; 30 fs
- ❑ 2 mm supersonic helium gas jet, ~10^{19} cm^{-3}

Table 1 | Statistics of the electron beam parameters over 20 shots

Peak energy (mean ± s.d.)	117 ± 7 MeV
Energy spread FWHM (mean ± s.d.)	11 ± 2 %
Charge (mean ± s.d.)	19 ± 6.8 pC
Beam divergence FWHM (mean ± s.d.)	5.8 ± 2 mrad
Beam pointing stability (mean ± s.d.)	0 ± 1.8 mrad

J. Faure, *et al., Controlled injection and acceleration of electrons in plasma wakefields by colliding laser pulses,* Nature, 444, 737 (2006).

Colliding pulse injection

- Experimental studies from University of Nebraska-Lincoln

➢ponderomotive drift, wake- wake interference, transverse laser interference

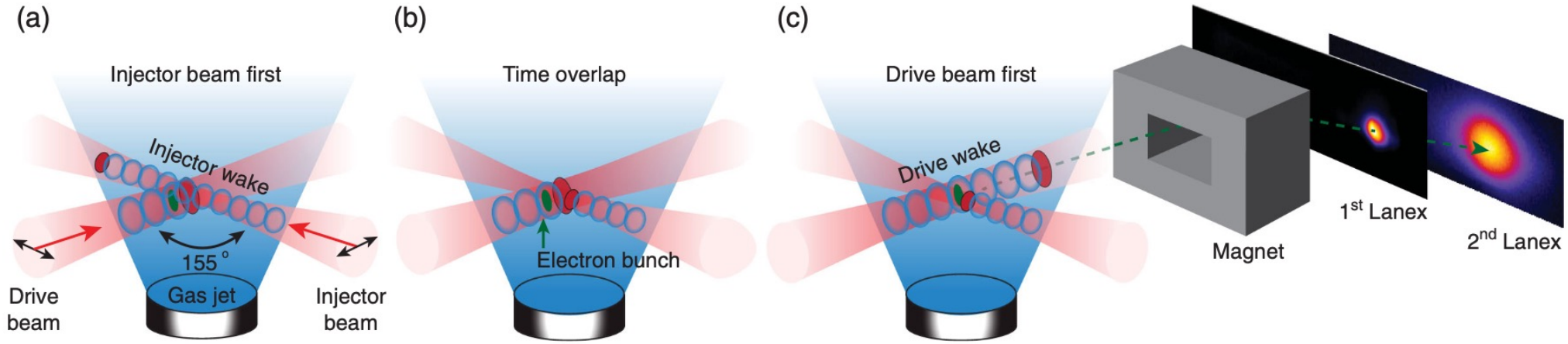

G. Golovin, *et al., Electron Trapping from Interactions between Laser-Driven Relativistic Plasma Waves,* Phys. Rev. Lett. 121, 104801 (2018); Q. Chen, et al., Transient Relativistic Plasma Grating to Tailor High-Power Laser Fields, Wakefield Plasma Waves, and Electron Injection, Phys. Rev. Lett. 128, 164801 (2022).

Free combinations

- Combinations between ionization injection, downramp injection and colliding pulse injection can produce several beamlets which are separated in space and/or energy. These beams may have critical applications.

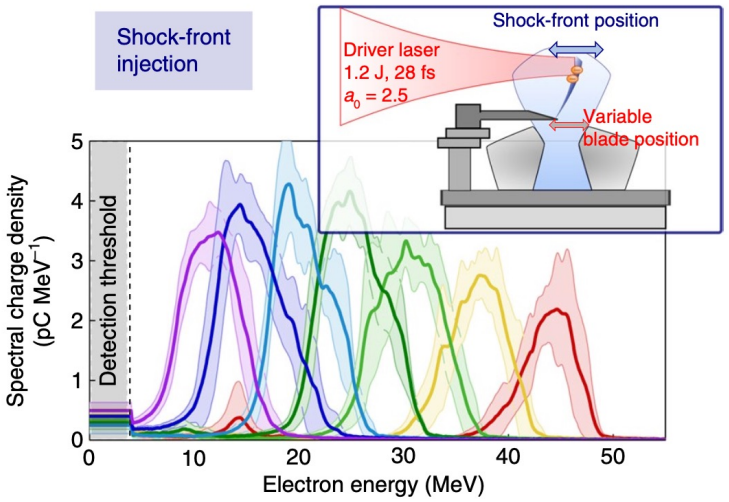

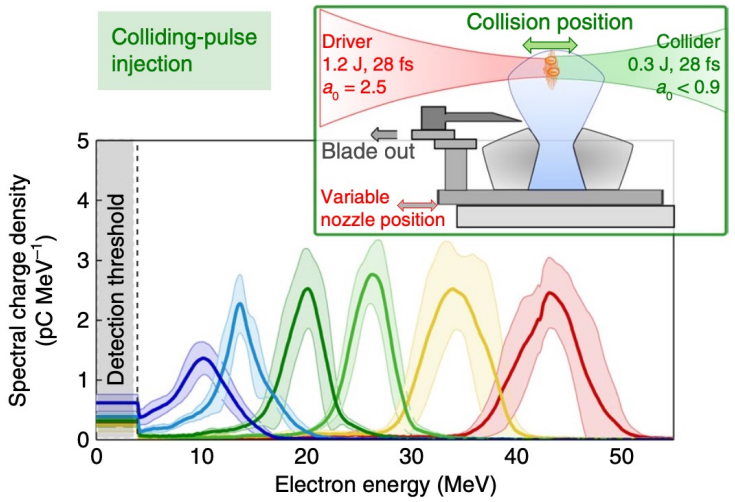

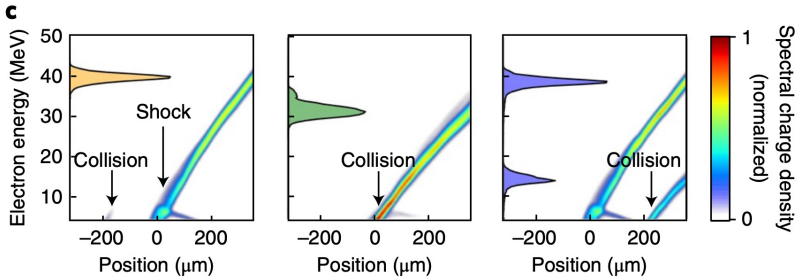

J. Wenz, *et al., Dual-energy electron beams from a compact laser-driven accelerator,* Nature Physics, 13, 263–269 (2019).